UC Berkeley
UC Berkeley Electronic Theses and Dissertations

Title
Tropical plant hydraulics in a changing climate: importance for species distribution and vulnerability to drought

Permalink
https://escholarship.org/uc/item/6jr828g9

Author
Fontes, Clarissa

Publication Date
2019

Peer reviewed|Thesis/dissertation

eScholarship.org Powered by the California Digital Library
University of California

Tropical plant hydraulics in a changing climate: importance for species distribution and vulnerability to drought

By

Clarissa Fontes

A dissertation submitted in partial satisfaction of the

requirements for the degree of

Doctor of Philosophy

in

Integrative Biology

in the

Graduate Division

of the

University of California, Berkeley

Committee in charge:

Professor Todd E. Dawson, Chair

Associate Professor Paul V.A. Fine

Professor Jeffrey Q. Chambers

Spring 2019

Abstract

Tropical plant hydraulics in a changing climate: importance for species distribution and vulnerability to drought

By

Clarissa Fontes

Doctor of Philosophy in Integrative Biology

University of California, Berkeley

Professor Todd E. Dawson, Chair

Amazonian droughts are becoming more frequent and intense, having a profound effect on water availability for plants. However, we still have limited abilities to predict the effect of climate change on plant species survival and distribution in mega-diverse systems like the Amazon. Plant hydraulic traits coupled with the assessment of environmental characteristics emerge as an important tool to assess species physiological performance and resilience, especially during extreme climatic events. Here we investigate plant hydraulic strategies and physiological performance of tropical tree species (***i***) across contrasting environments, (***ii***) during an extreme drought event and (***iii***) during the course of a day to understand how water availability may shape species distribution and plant vulnerability to drought in the Amazon Basin.

In the first chapter, I investigate if the current patterns of species' distribution in the main Amazonian habitats can be explained by species hydraulic strategies and how variation in the hydraulic properties of Amazonian forests influences species-specific vulnerability to drought across different habitat types. I found strong segregation between species from wet vs. dry environments in relation to their functional traits, suggesting that water availability could be a strong predictor of species functional composition in the different Amazonian environments. Also, the xylem of dry-habitat species are more embolism resistant, but it may not be correct to assume that these species will be the ones performing better under a warmer and drier climate.

The second chapter assesses plant physiological performance during a strong El Niño. This is the first study in the Amazon to measure *in situ* tree physiological stress before, during and after a natural drought event. I show that the warmer and drier conditions imposed by the El Niño greatly amplified trees' physiological stress and could affect growth, phenology and potentially lead to tree mortality. Given the extreme nature of the this El Niño and that temperatures are predicted to increase in the tropics, this work can serve as a case study of the possible impact climate warming can have on tropical trees.

In the third chapter, I analyzed the diurnal patterns of stomatal conductance, water potential, and sap velocity during the dry season and investigate how they change with

canopy temperature and vapor pressure deficit. I found that unlike preview reported, plants have a re-hydration period during the hottest time of the day probably due to an imbalance between stem sap-velocity and leaf transpiration rates. This study helps to elucidate the array of processes influencing diurnal patterns of plant-water balance in tropical trees.

DEDICATION

To my parents Ruy and Eliana for all their love and support.

TABLE OF CONTENTS

Abstract ……...1
Dedication ……..…...i
Table of Contents ……..…...ii
Acknowledgments ……iii

Chapter 1. Convergent evolution of tree hydraulic traits in Amazonian habitats: implications for community assemblage and vulnerability to drought

Abstract ……...1
Introduction ……1
Materials and Methods ……3
Results ……8
Discussion ……...9
Reference ……..12
Figures ……...19

Chapter 2. Dry and hot: the hydraulic consequences of a climate change-type of drought for Amazonian trees

Abstract ……25
Introduction ……..25
Materials and Methods ……26
Results ……..30
Discussion ……....32
Reference ……..36
Figures ……...41

Chapter 3. A recovery in leaf water potential during midday in Amazonian trees is driven by an imbalance between water demand and supply

Abstract ……47
Introduction ……..47
Materials and Methods ……48
Results ……..50
Discussion ……51
Reference ……..54
Figures ……..57

ACKNOWLEDGEMENTS

I thank Todd Dawson and Jeffrey Chambers for the thoughtful guidance, support, and wonderful friendship. I also thank Paul Fine for many invaluable discussions that have improved my research and the path of my career.

I have been very fortunate to have the most amazing Lab mates. I thank Claire Willing, Roxy Cruz, Ilana Stain, Kelsey Crutchfield, Sue Pierre, Anthony Ambrose, Wendy Baxter, Leander Anderegg, Robert Skelton, Adam Rody, Cameron Williams and Allison Kidder, Stefania Mabelli for being stellar human beings, awesome friends and marvelous scientists.

I would like to thank my collaborators in Manaus-Brazil, Niro Higuchi, Bruno Gimenez, Raquel Fernandes, Flávia Durgante, Caroline Lara, Livia Naman, Livia Granadeiro, Caique Celes, Kolby Jardine and Gabriel Ribeiro for their support and friendship. Especially, I thank Matapi for the amazing assistance in the field.

I have had the privilege of pursuing the questions and ideas that I felt most interesting and important. I thank Science Without Borders, NGEE-Tropics, UC Berkeley- Integrative Biology, Berkeley International Office and UC Berkeley Graduate Division for their financial support.

None of this would have been possible without the unconditional love and support of my parents Ruy and Eliana Fontes. My mom has inspired my curiosity about the natural world. From her, I inherited the passion for traveling and the courage, and excitement for living new experiences. My dad has always been and will always be my safe harbor. To me, he is an example of kindness, loyalty, and emotional strength. I also want to thank my brother, Augusto Fontes, for being that peaceful and sensitive human being, always there when I needed.

I do not imagine doing this without Gabriel Damasco, my partner, by my side. I want to thank him for making the good moments even happier and the turbulent moments easier to navigate. I thank Miguel Vale, my son, for being the sunshine in my life and teaching me that the most valuable things in life are invisible to the eye.

CHAPTER 1 Convergent evolution of tree hydraulic traits in Amazonian habitats: implications for community assemblage and vulnerability to drought

Abstract

Amazonian droughts are becoming more frequent and intense, having a profound effect on water availability for plants. However, little is known about how variation in the hydraulic properties of Amazonian forests influences species-specific vulnerability to drought across different habitats types. Here we ask if ***(i)*** the current pattern of species' distribution in the main Amazonian habitats (flooded, valley, plateau, and white-sand forest) can be explained by species hydraulic strategies, ***(ii)*** if species from dry vs. wet environments differ in their vulnerability to embolism that would compromise their ability to transport water, and ***(iii)*** if wet-habitat species are more vulnerable to hydrological droughts than dry-habitat species. To answer these questions we measured 16 traits from 16 congeneric species distributed in four Amazonian habitats. We found strong segregation between species from wet vs. dry environments in relation to their functional traits, and hydraulic characteristics (e.g vessel hydraulic diameter and hydraulic conductivity) were the main traits driving this pattern. Thus, water availability can be a strong predictor of species functional composition in the different Amazonian environments. The P_{50}s (water potential when plant loose 50% of its conductivity) of dry-habitat species were significantly more negative (47.7%) than wet-habitat species. However, we did not see any difference in stem safety margin between species from different environments. Therefore, the xylem of dry-habitat species are more embolism resistant, but it may not be correct to assume that these species will be the ones performing better under a warmer and drier climate.

Introduction

The Amazon Basin occupies an area of approximately 7 million Km^2 and is the largest and most biodiverse tropical rainforest in the world (Ribeiro *et al.*, 1999). The main vegetation types found in the Amazon Basin are mature *terra-firme* forests (plateau and slope forests; ~ 63% of Amazon Basin), woodland savanna/white-sand forests (~24.5%), floodplain/inundated forests (4.2%), and grass-dominated areas (~ 4.8%; Saatchi *et al.*, 2007). These distinct habitats mainly differ in soil type, plant water availability, and topography. This great environmental heterogeneity has been proposed as one of the main explanations for the high diversity of tree species in Amazonian tropical ecosystems (Connell, 1978; Smith *et al.*, 1997; ter Steege *et al.*, 2000). Environmental hetereogeneitty can promote ecologically-mediated speciation and habitat specialization and thus, increase beta-diversity among areas (Tuomisto *et al.*, 2003; Fine & Kembel, 2011; Fine, 2015; Leibold & Chase, 2017). Indeed, several studies have reported high tree species turnover in the different Amazonian habitats (e.g. ter Steege *et al.*, 2000; Valencia *et al.*, 2004; Stropp *et al.*, 2011; Schietti *et al.*, 2014). And a large number of studies have tested for edaphic and topographic habitat specialization among

tropical trees (e.g. Phillips *et al.*, 2003; Fine & Kembel, 2011; Damasco *et al.*, 2013; Toledo *et al.*, 2017). However, despite the strong differences in plant water availability among these diverse Amazonian habitats, relatively little attention has been paid to how this water availability, or limitation, can be linked to tree species distribution and Amazonian megadiversity (but see Schietti *et al.*, 2014; Oliveira *et al.*, 2019), which is particularly important to understand in face of the rapid climatic and land-use change currently taking place in the Amazon Basin.

Extreme drought events are becoming more frequent and intense in the Amazon Basin (Jenkins *et al.*, 2010; Marengo *et al.*, 2011; Fu *et al.*, 2013; Stocker *et al.*, 2013) and many studies have linked warmer and drier conditions to increased levels of tree physiological stress in tropical areas (Doughty & Goulden, 2008; Bonal *et al.*, 2016; Fontes *et al.*, 2018b; Tng *et al.*, 2018). Precipitation is also predicted to decrease across the Amazonian region (Stocker *et al.*, 2013), and if true, this will have profound effects on water availability for trees. Water is an essential resource for plants and contrasting environments with distinct levels of water availability may select species that have different hydraulic strategies (Engelbrecht *et al.*, 2007; Blackman *et al.*, 2014; Cosme *et al.*, 2017). Some studies have suggested that inundated forests of the Amazon Basin may be more vulnerable to hydrological droughts than plateaus species (Zuleta *et al.*, 2017; Oliveira *et al.*, 2019). However, the physiological mechanism for this assertion has not been fully explored and the drought vulnerability of species from different Amazonian habitats has yet to be tested. Thus, if we are to understand the effect of future climate in the biggest tropical forest in the world, it is of paramount importance to know how water limitation may shape species distribution in the contrasting Amazonian habitats, and how these communities differ in their vulnerability to water deficit.

Hydraulic traits such as P_{50} (the water potential at which plants lose 50% of their hydraulic conductivity) and stem safety margin (SM; how close the plant is to reaching its P_{50}) are widely used to assess vulnerability and response of plants to drought (Choat *et al.*, 2012; Skelton *et al.*, 2015; Fontes *et al.*, 2018b). They have also been shown to influence plant growth, fecundity and survival rates (Poorter *et al.*, 2010; McDowell, 2011; Fan *et al.*, 2012). Hydraulic traits can be particularly important in delineating the carbon uptake and water loss trade-offs and life-history strategies that influence population demographics and species distribution across environmental gradients (McGill *et al.*, 2006; Anderegg *et al.*, 2014). However, we have little knowledge about hydraulic trait variation across tropical rainforest tree taxa. Therefore, the Amazon is still underrepresented in global plant hydraulic trait datasets, probably because of the high species diversity, the difficulties in accessing remote areas, and the fact that hydraulic traits are time-consuming to quantify.

In the study presented here we measured 16 leaf, wood and hydraulic traits of 16 congeneric trees species exhibiting contrasting distributions across four main Amazonian habitats, making this study 2 times larger than previous research on plant hydraulic strategies in the Amazon. We selected two environments where water is constantly available throughout the year (flooded and valley forests) and another two habitats where water is limited during the dry season (white-sand and plateau forests) to test the following hypothesis: **(*i*)** Amazonian trees occurring in wet habitats (flooded and valley forests) are more vulnerable to xylem embolism than species from dryer environments (plateau and white-sand forest); **(*ii*)** Despite the differences in xylem vulnerability to

embolism between wet and dry habitats, stem hydraulic safety margins across the four environments will not be significantly different; ***(iii)*** Sister species from contrasting environments in the Amazon will differ in their leaf, wood and hydraulic traits. We hypothesize that these trait differences evolved repeatedly and independently in the distinct close phylogenetic lineages due to selective environmental pressure (ecological speciation).

Materials and Methods

Study site

The study was conducted in two areas, Reserva Biológica do Cuieiras/Estação Experimental de Silvicultura Tropical, also known as ZF-2 (2°36'33''S, 60°12'33''W), and at the Uatumã Sustainable Development Reserve (USDR) where the Amazon Tall Tower Observatory, ATTO, is situated (2°08'38''S, 58°59'59''W). The ZF-2 and ATTO are located, respectively, ~90 km northwest and ~150 km northeast of the city of Manaus-AM, Brazil. The ZF-2 site has 31000 ha of dense humid *terra-firme* forest, with a mean canopy height of approximately 28m (Roberts *et al.*, 1996; Kunert *et al.*, 2017). The mean annual precipitation between 2002 and 2016 was 2140 mm, and the mean annual temperature was 28.17 ºC (Fontes *et al.*, 2018b). The ATTO site, consists of several forest ecosystems. Upland *terra-firme* forests (plateaus) are found on higher altitudes (approximately 130m a.s.l.), while seasonally flooded black-water forests (*igapó*) dominate along the main river channel. White-sand forests (*campinarana*) are found between the river terraces and the plateau (approximately 35-45 m a.s.l). The annual average precipitation and temperature between 2012 and 2014 were respectively, 2376mm and 28ºC. The dry season for both areas is between July and September when precipitation is below 100mm. For more information about ZF-2 site description refer to Fontes *et al.* (2018a); Fontes *et al.* (2018b) and for ATTO see Andreae *et al.* (2015); Targhetta *et al.* (2015).

We measured 16 leaf, wood and hydraulic traits (Table 1) of 16 species (11 congeneric species) occurring in four contrasting environments: flooded forest, valley, plateau and white-sand forest (Figure 1). Flooded forest (FF) and white-sand forest (WS) species were sampled in the ATTO site, while valley (V) and plateau (P) species were sampled at the ZF-2 reserve. Therefore, each site has a wet (FF or V) and a dry (P or WS) environment. These four habitats cover the main gradients of soil texture, fertility, water availability (water table depth) and forest structure found in the Amazon Basin. The soil texture in the flooded black water forests of Uatumã river is predominantly clay and are nutrient poor with pH values (H_20) of 4.05 ± 0.2 (Targhetta *et al.*, 2015). These forests have a low tree species richness with 26-49 species ha^{-1} and the mean flood height is 2.77 ± 0.9 m for up to 230 days $year^{-1}$ (Table S1; Andreae *et al.*, 2015). Valley habitats are the lower riparian areas with the sand content in the soil varying from 77 to 83% (Ferraz *et al.*, 1998). Valleys are mostly flat with the water table close to the surface (up to 1 m deep) and soils are seasonally waterlogged during the rainy season (Tomasella *et al.*, 2008). Plateaus are generally flat or have gentle slopes (<7%) with altitude varying between 90 and 120 m. The soils have a high concentration of clay (80-90%), are well drained, and the water table is c. 20 m deep (Tomasella *et al.*, 2008). Finally, the white-

sand forests are characterized by nutrient-poor soils with high acidity (Targhetta *et al.*, 2015). Sand content in the soil is high, 93.3 ±1.5% and water table depth can reach 4m deep. White-sand forests have a high incidence of solar radiation and leaf temperature can be 3-5^{o}C higher than in plateau forests (Medina *et al.*, 1978; Rinne *et al.*, 2002). This habitat can become very dry and hot during the dry season. In summary, the main environmental differences between the four habitats are soil texture/fertility and water availability (water table depth), as shown in Figure 2. Also, FF and V areas have little water constraints (water is available throughout the year), while P and WS habitats are more water limited and can experience very low water conditions during the dry season. For more information about the differences in forest structure among the four environments refer to Table S1 in the supplemental information.

Environmental Variables

We used soil texture (clay and sand percent), and water table depth (minimum and maximum) to characterize soil and water availability in each of the plots where the individual trees were collected (Figure 1). Water table depth for the ZF-2 site from 2014 to 2016 was provided by the LBA Hydrology group. The raw data is available upon request to the LBA Hydrology group through the link: https://docs.google.com/forms. Soil texture data for ZF-2 were obtained from Ferraz *et al.* (1998). For the ATTO site, data of water table depth and soil texture were extracted from previous studies (Andreae *et al.*, 2015; Targhetta *et al.*, 2015).

Species selection

The species were selected from the database of permanent plots (diameter at breast height ≥ 10 cm) located at ATTO (Targhetta *et al.*, 2015) and ZF-2 reserve (Fontes *et al.*, 2018a; Fontes *et al.*, 2018b). Sixteen tree species (Figure 1) were sampled to answer hypothesis *i* and *ii*. A subset of these species, being 3 congeneric triplets (*Eschweilera, Swartzia, Protium*) and 1 congeneric pair (*Licania*; 11 species at total), were used to investigate hypothesis *iii* (Figure 1). Fifteen out of the sixteen species are included in the 10 most abundant families in these two regions (Burseraceae, Chrysobalanaceae, Fabaceae, Lecythidaceae, and Sapotaceae) and have distributions mostly restricted to one of the four environments. For the congeneric dataset, we have at least one species from each genus occurring in a wet (FF or V) and a dry habitat (P and WS; Figure 1).

Trait selection

Stomatal density and specific leaf area: Stomatal imprints were obtained by applying clear nail polish on the abaxial surface of fully expanded and mature leaves. After 3-5 minutes drying period, the impressions were peeled off the leaves, placed on microscope slides and embedded in glycerin for examination. Leaf imprints were examined at x400 magnification using a Leica DM2500 light microscope (Leica Microsystems Vertrieb GmbH, Wetzlar, Germany) and stomatal density was determined. A digital camera (Nikon digital sight, DS-Fi1) attached to the microscope was used to

take a photo of the analyzed impression areas. Three plants per species, three leaves per plant and three photos/areas per leaf were examined.

Specific leaf area (SLA; $cm^2\ g^{-1}$) was estimated as the ratio of fresh leaf area to leaf dry mass. Leaves were collected between 7:00h and 9:00h, and immediately placed in plastic bags with a moist paper towel. Fresh leaf area was measured using a portable leaf area meter (CI-202 CID Inc., Cama, WA, EUA) after ~2 hours of being collected. The leaves were dried at 60ºC for 72 h and their dry mass was measured with an analytical balance (0.001g precision). Three to five plants per species and 7-10 leaves per tree were measured.

Carbon and nitrogen isotope composition: leaves were oven dried at 60ºC for 72h and then grounded to a fine powder. Powder of dried leaves was analyzed for N and C stable isotope abundances using elemental analyzer/continuous flow isotope ratio mass spectrometry haused in the Center for Stable Isotope Biogeochemistry at the University of California Berkeley, USA. Analyses were performed using a CHNOS Elemental Analyzer interfaced to an IsoPrime100 mass spectrometer. Long-term external precision for C and N isotope ratio analyses are ± 0.10‰ and ± 0.20‰, respectively. Abundances measured are denoted as δ values and are calculated according to the equation:

$$\delta^{13}C \text{ or } \delta^{15}N = (R_{sample} / R_{standard} - 1) \times 1000\ [‰]$$

R_{sample} and $R_{standard}$ are the ratios of heavy-to-light isotopes of the sample and the respective standard.

Wood specific gravity and xylem anatomy: to measure the wood specific gravity (WSG; $g\ cm^{-3}$), for each tree we collected three branch fragments in the last growth unit with a diameter of ~ 1 cm and a length of ~5 cm. Outer bark and pith wider than 1mm in diameter were removed. Branch samples were saturated with water overnight and saturated volume was estimated using the water displacement principle. Briefly, branches were immersed in a beaker with water located on top of an analytical balance (0.001g precision). The wood sample was placed just below the water surface with the aid of a needle. The volume of the wood was estimated as the mass of displaced water (Williamson & Wiemann, 2010). After measurement of the saturated volume, samples were dried at 101-105 ºC for 72 h and dry mass was determined. Branch specific gravity was measured as the dry mass divided by the saturated volume. Three to five plants per species and three branches per plant were measured.

For anatomical trait measurements, we collected one branch per tree and three individuals per species from 11 species (3 congeneric triplets and 1 congeneric pair). Each branch fragment was harvested from the last growth unit and had a diameter of 1-2 cm. Branches were placed in plastic vials and stored in cooler with ice until they were transported to the field station (30 min to 1 h after being collected) where they were frozen for tissue preservation. Before we started the anatomical procedure, samples were slowly thawed in water and in the fridge overnight. We cut cross-sections (20–30 lm thick) for each branch sample with a rotary microtome (Spencer 820, American Optical, Buffalo, NY). Cross-sections were stained in 0.5% Toluidine Blue for 10 minutes and rinsed. Cross-sections were dehydrated in ethanol series at 50% (for 1 min), at 75% (for 3 min) and at 100% (for 5 min) before mounting. Up to eight cross-sections per sample were embedded in glycerin for histological examination. We selected one cross-section

per sample and used a digital camera (Nikon digital sight, DS-Fi1) mounted on a light microscope (Leica DM2500, Wetzlar, Germany) to shoot three photographs with APO x10 lens, covering different parts of the cross-section, allowing the estimation of the variability in vessel size. Image analyses were conducted with ImageJ – Fiji4 (https://imagej.net/Fiji/Downloads). For images with good contrast, we performed an automated delimitation of the vessels with a threshold function in Fiji. For those with lower contrast, we manually filled the vessel areas. Anatomical traits measured in the three photographs of each branch sample were then averaged to determine individual values. For each image, we measured individual vessel area (to estimate mean vessel area = *VA*; μm^2), vessel diameter (*D*), and counted the total number of vessels per unit area (vessel density = *VD; n* μm^{-2}). Vessel diameter was estimated as $D = (D_1 + D_2)/2$, where D_1 is the maximum vessel diameter and D_2 is the minimum vessel diameter in µm. We calculated three metrics of hydraulic efficiency, vessel function as $VF = VA \times VD$; the ratio between size and number of vessels, $S = VA/VD$; and the mean vessel hydraulic diameter (µm), $D_{mh} = (\sum D^4/n)^{1/4}$ where *n* is the total number of vessels in an image (Zanne *et al.*, 2010; Scholz *et al.*, 2013).

Water potential, xylem resistance to embolism, leaf hydraulic conductivity and stem conductance: midday water potential (Ψ_{midday}; MPa) was measured at least once a month during the peak of the 2015 dry season (August-October) between 11:30h and 13:30h using a Scholander pressure chamber (PMS, Corvallis, OR, USA; accurate to 0.5 MPa; Scholander *et al.*, 1965). Three full-developed sun shoots (2-5 leaves) per plant and three to five plants per species were sampled. Shoots were harvested, immediately wrapped in a damp paper towel, aluminum foil and bagged in separate zip-lock with a moist paper towel to avoid further water loss. For each shoot, the assessment of xylem water potential was made c. 5 min after the leaves were collected.

We used P_{50} (the water potential at which 50% loss of hydraulic conductivity occurs) and stem hydraulic safety margin (SM) as indicators of xylem vulnerability to hydraulic failure. SM was calculated as $SM = P_{min} - P_{50}$, where P_{min} is the minimum stem water potential measured during the dry season of 2015 (August-October). We measured P_{50} for branches of mature trees with stem diameters between 15-25 cm. For each of the 16 species, we collected 3 sun-exposed branches from 3-5 individuals. The branches were longer than the maximum vessel length measured for the species. Maximum vessel lengths were measured in a minimum of 3 individuals per species (Jacobsen *et al.*, 2007) and varied from 29-87cm in FF, 46-57cm in V, 8.5-77cm in P and 18-56cm in WS forests. Hydraulic vulnerability curves were constructed using the bench dehydration method (Sperry *et al.*, 1988) using an ultra-low-flow meter (Pereira & Mazzafera, 2012; Pereira *et al.*, 2016). Branches were air-collected early in the morning (5:30 – 6:30 AM local time) and were transported to the field station in dark plastic bags after 30 min-1 hours after being collected. Branches were bench dried for different amount of time (0 min to 3 hours) and placed in dark plastic bags for 2 – 8 hours so leaf and xylem water potential would equilibrate. A total of 2-3 leaves from each branch were used to estimate water potential. The branch was then cut under water into 5 segments (4-5 cm long each and ~ 1cm were shaved off each end), connected in series to the hydraulic apparatus and initial conductance was measured (Pereira *et al.*, 2016). The tension of the branches was relaxed prior to excising the segment on which measurements were performed. Branches

were then flushed for ~25 min at 100 kPa with 20 mM KCL solution, filtered to 0.1 µm (inline filter; GE Water and Process Technologies, Trevose, PA, USA) and vacuum-degassed for at least 1 hour. After flushing, the maximum conductance of the same branch segments was assessed. The percent loss of hydraulic conductivity (PLC) was measured for each of the segments using the hydraulic conductance measurements taken before and after the flushing.

The same apparatus and solution used to assess hydraulic vulnerability curves (Pereira & Mazzafera, 2012; Pereira *et al.*, 2016) were employed to measure native stem hydraulic conductivity and leaf specific conductivity (respectively k_h and k_{leaf}). To determine k_h and k_{leaf}, we air-collected one branch per tree and three individuals per species from 11 species (3 congeneric triplets and 1 congeneric pair). Branches 2-3x longer than the maximum vessel length measured were collected at predawn and immediately placed in double-plastic-bags containing a wet tissue paper to minimize post-cutting dehydration. A total of 2-3 leaves from each branch were used to estimate water potential. Branches were cut under water, trimmed, connected to the hydraulic apparatus and stem hydraulic conductivity (k_h) was measured (Pereira & Mazzafera, 2012). The distal diameter of these segments varied from 2 to 4mm and they were 0.4 to 1.10 m in length. All leaves located distally from the measured branch were collected and their area was calculated using a portable leaf area meter (CI-202 CID Inc., Cama, WA, EUA). k_{leaf} was calculated as k_h divided by the total leaf area of the branch (Venturas *et al.*, 2016).

Statistical analysis

To evaluate if species occurring in contrasting environments differ in their vulnerability to hydraulic failure we performed an ANOVA with P_{50} and SM values, using the four different environments as treatments. We used the post-hoc Tukey Honest Significant Difference test (Tukey HSD) to identify which habitats were different from one another. The Tukey HSD test was used instead of the regular *T*-test because it allows treatments to have uneven sample sizes (number of species sampled in each environment was not always the same). A principal component analysis (PCA) was used to evaluate the difference in soil texture and water table depth between the 52 plots where the species were sampled. PCA was also used to assess the patterns of covariation between traits and to describe hydraulic strategies of species in different environments. We used ANOVA and Tukey HSD with the mean value of species traits to determine if species from the same genus occurring in contrasting environments differed in their leaf, wood, and hydraulic traits. We used the Shapiro-Wilk normality test to check if traits had a normal distribution. Traits that did not meet the assumptions of a normal distribution ($N_{stomata}$, k_{leaf}, k_h, C:N ratio, VF, S:N ratio, D_{mh}, VA) were log-transformed.

We built a phylogenetic tree for our species using the backbone phylogeny of APG III (R201208029) available in Phylomatic v.3 (Webb & Donoghue, 2005). Branch-lengths were estimated using Grafen's transformation (Grafen, 1992). Analyzing species within clades allows for a phylogenetically independent contrast, nevertheless we tested for a phylogenetic signal of all traits using the Blomberg *K* (Blomberg *et al.,* 2003) and Pagel lambda (Pagel, 1999), with significance tested by 999 permutations. For all statistical analyses, we used R v.3.3.0 with base packages (R Core Team, 2014).

Results

Xylem resistance to embolism formation (P_{50}) ranged from -0.59 to -2.1 MPa across species (Figure 3, Figure S1). Species from wet environments, such as valley (V) and flooded forests (FF), had similar P_{50} values (Tukey HSD test, *p*-value = 0.74) but these species were also significantly more vulnerable to xylem cavitation (47.7% higher P_{50} values) than species from plateau (P) and white-sand forests (WS; Tukey HSD test, *p*-value < 0.01). The only exception was the FF species *Eschweilera tenuifolia* which had a P_{50} of -2.1 MPa (Figure 3b). Despite the differences in embolism formation between wet and dry habitats, xylem hydraulic safety margins (SM) across the four environments were not significantly different (Figure 4; ANOVA test, *p*-value = 0.324). Also, we found that all the studied species operated with very narrow (< 1 MPa) safety margins, indicating that regardless of their water availability, the different Amazonian habitats can be equally vulnerable to extreme droughts. A similar result was found when a more conservative hydraulic safety margin was used ($SMP88 = P_{min} - P_{88}$; Figure S2).

Species from wet (FF and V) and dry (P and WS) environments differed in most of their leaf, wood, and hydraulic traits. Furthermore, these trait values were not significantly different between FF and V or P and WS (Table S2), indicating a convergence of these functional traits based on environment water availability. Wet habitat species had significantly higher values of SLA (29.7% higher), C:N ratio (15.8%), Ψ_{midday} (43.3%), P_{50} (47.7%), k_{leaf} (80.9%), k_h (71.5%), Dmh (8%) and VA (15% higher), while drier environments had higher value of WSG (2% higher; Figure 5). The number of stomata, vessel fraction (VF), vessel size: number ratio, xylem safety margin, stem hydraulic conductivity, δ^{13} C and δ^{15}N did not differ significantly between the congeneric species occurring in the four contrasting environments (Table S3). Species mean, minimum and maximum values of the sixteen functional traits are shown in Table S3.

The first PCA component explained 39.9% of all variation and was dominated by VA, Dmh, k_{leaf} and k_h, Ψ_{midday}, P_{50}, SLA (Figure 6). The second axis accounted for 17.3% more of the variation and was mainly controlled by WSG and C:N ratio (Figure. 6). Thus, the score of the species on the first axis is a composite of wood anatomical and stem/leaf hydraulic traits where high scores indicate high values of VA, Dmh, k_{leaf}, k_h, Ψ_{midday}, P_{50}, SLA, and low scores indicate opposite traits. The second axis reflects wood density and resource acquisition vs. protection, and high scores indicate denser wood while lower scores are associated with higher C:N ratio. FF and V species were mostly grouped in the right side of the PCA space, with the exception of the species *E. tenuifolia* which is found in FF but have a high vulnerability to embolism formation. P and WS species were located in the left side of the PCA space. Furthermore, this pattern was mainly driven by hydraulic traits, suggesting the importance of water availability for species distribution in the tropics (see Table S3 for loadings of PCA 1 and 2). Finally, there was no phylogenetic signal for any of the 16 traits analyzed in this study (K ranged from 0.18 to 0.43 and λ from 7.082 e^{-5} to 0.57; Table S2), indicating that these traits are not conserved in the phylogeny. These results show that species from wet habitats are more similar to each other than they are to their sister species growing in drier environments.

Discussion

Our study reveals that xylem embolism resistance varies significantly between wet and dry environments at small spatial scales within four Amazonian habitats. However, we show for the first time, that across Amazonian tree species regardless of the environment they currently occupy and its water availability, operate at narrow safety margins (SM; < 1 MPa), indicating that the studied species may be equally vulnerable to extreme drought events. We also found that congeneric species were not grouped together in relation to their leaf, wood and hydraulic traits. Instead, species from wet habitats, such as FF and V, were more functionally similar to one another than to their congeneric species growing in the adjacent dry environments (P and WS forests). Our results suggest that these differences evolved repeatedly and independently in the distinct close phylogenetic lineages due to selective environmental pressure.

Embolism resistance and hydraulic safety margins

We found that species from P and WS forests have significantly lower P_{50} and P_{88} values than their congeneric species growing in V and FF (Figure. 3 and Figure S2). This result supports the idea of an increase in xylem cavitation resistance as water availability decreases (Santiago *et al.*, 2018; Oliveira *et al.*, 2019). Low values of P_{50} and P_{88} can be linked with low xylem efficiency but high xylem safety (Sperry *et al.*, 2008; Gleason *et al.*, 2016) and they are frequently used to compare different species' vulnerability to water deficit (e.g. Powell *et al.*, 2017; Santiago *et al.*, 2018; Oliveira *et al.*, 2019). In V and FF habitats the water table is close or even above the surface, suggesting water is constantly available for plants. Since it is energetically costly to build wood and leaf tissues that are resistant to water deficit (van Gelder *et al.*, 2006; Sobrado, 2009), it may not be advantageous for species growing in these environments to invest in a safer hydraulic system. Thus, plants that have a greater hydraulic efficiency may be stronger competitors in these habitats, while trees that have slow resource acquisition characteristics may be selected against or outcompeted from these wet environments. On the other hand, species found in P and WS areas may need to tolerate higher xylem tension to be able to establish in drier habitats. In plateau areas the water table is deep (~ 20m deep) and plants have to rely on a resistant hydraulic system or on deeper roots to be able to preserve or acquire water during the dry season (Brum *et al.*, 2018; Oliveira *et al.*, 2019). In white-sand forests, the water table is not very deep as in P areas (~ 4m deep) and it can even get waterlogged during the rainy period. However, during the dry season the sandy soils dry out quickly and in combination with high solar radiation can cause plants to experience extreme water stress (Targhetta *et al.*, 2015; Zanchi *et al.*, 2015).

P_{50} and P_{88} values only provide us with information about the water potential at which plants have lost 50% of their hydraulic conductivity due to xylem cavitation (Bucci *et al.*, 2016; Santiago *et al.*, 2018). However, to know when or how close a particular plant species is to reaching that level, we need to have midday water potential data from the field, to be able to calculate xylem hydraulic safety margin ($SM = P_{min} - P_{50}$). Narrow SM can benefit plants by allowing the maintenance of gas exchange under a more negative xylem tension (Brodribb & Holbrook, 2004; Sperry, 2004). Yet, species with such SMs are at a higher risk because narrow SMs make them more vulnerable to

water deficit like those that would occur during a severe or unusual drought events. Thus, the knowledge of SM may be more informative than only documenting xylem vulnerability to cavitation because, SMs indicate how close a plant operates to the loss of its hydraulic capacity (Meinzer *et al.*, 2009; Bucci *et al.*, 2016). Indeed, we found that despite the differences in vulnerability to embolism between wet and dry habitats (Figure 3), SMs across the four environments were not significantly distinct (Figure 4). A similar pattern was documented in a global analysis by Choat *et al.* (2012), suggesting that the same processes driving large scale patterns of xylem vulnerability and SMs are also operating at local and regional scales. Therefore, water availability seems to be a strong environmental constraint on species distribution across the Amazonian habitats and only species with high embolism resistance (low P_{50}) can survive in drier environments. However, it may not be correct to assume that these species will be the ones performing better or less likely to die from hydraulic failure under a warmer and drier climate.

We found that some species from FF (*Swartzia laevicarpa*), P (*Protium hebetatum*) and WS (*Swartzia acuminata*) were operating under negative safety margins (with less than 50% of its hydraulic conductivity; Figure 4), suggesting these species were experiencing some degree of water stress during the time of data collection. During our study, the most severe drought registered in the last decade hit Central Amazon, with profound effects on plant physiological performance (Fontes *et al.*, 2018b). Our results indicate that this drought amplified the degree of trees' physiological stress in trees from across all the main Amazonian habitats. It also corroborates the idea that species from wet and dry environments are equally vulnerable to changes in climate. Finally, even though the difference in SM among the four environments were not statistically significant, we did observe a trend in increasing SM with a decrease in water availability (Figure 4). More research on the patterns of xylem vulnerability and SMs across the different environments in the Amazon is needed before broad conclusions can be made.

Leaf, wood and hydraulic traits across contrasting Amazonian habitats

We found a strong trait variation between wet (FF and V) and dry (P and WS) Amazonian ecosystems. Species from P and WS forests were more functionally similar to each other than to their sister species growing in neighboring FF or V areas. This result was surprising, especially because WS and P forests are very different habitats and therefore could have very distinct selective pressures. Plateaus have much higher % of clay in the soil, higher nutrient availability, trees are taller (canopy height of ~ 30m) and the understory has lower solar radiation and higher relative humidity (Fine *et al.*, 2006; Baraloto *et al.*, 2011; Stropp *et al.*, 2011; Fortunel *et al.*, 2012; Damasco *et al.*, 2013; Stropp *et al.*, 2014). Thus, the fact that P and WS forests were not significantly different in any of the hydraulic traits measured in this study, reinforce the idea that water availability can be a strong predictor of species functional composition (Fortunel *et al.*, 2013; Cosme *et al.*, 2017; Medeiros *et al.*, 2018).

Species from dry environments had a higher leaf mass per unit area (lower SLA), lower wood specific gravity (denser wood) and C:N ratio than their sister species from wet areas (Figure 5 a, b and i). These results suggest that dry-habitat species may invest more in tissues that enhance the retention of captured resources, protection againts herbivores, mechanical strength and/or longer leaf life-spans (Reich *et al.*, 1997;

Westoby, 1998; Fortunel *et al.*, 2013; Kunstler *et al.*, 2016) than their congeneric species from wet environments. In contrast, species from FF and V areas had a bigger vessel area and wider vessel hydraulic diameters (Figure 5e-f). According to the Hagen-Poiseuille equation, the flow rate of water in the xylem should be proportional to the fourth power of its radius. Furthermore, while narrow vessels may be either vulnerable or resistant to cavitation, wide conduits tend to be vulnerable (Hacke *et al.*, 2017). Thus, wider vessels can transport water more efficiently and allow plants to acive higher hydraulic conductivity but, it also makes them more vulnerable to water stress (higher risk of xylem cavitation; Figure 5c-h; Sperry *et al.*, 2006; Gleason *et al.*, 2016; Hacke *et al.*, 2017). These results are consistent with the findings of Cosme *et al.* (2017) who reported similar trait combinations for species associated with valley vs plateau habitats. Therefore, our results suggest that species from wet Amazonian habitats have a tendency to possess more "fast-resource-acquisition strategies", *sensu* Reich (2014) while trees in the dry environments have traits that enhance resistance and resource conservation.

We acknowledge that the traits measured in this study may not represent all of the most important traits underlying habitat partitioning (Fortunel *et al.*, 2013; Fortunel *et al.*, 2014; Díaz *et al.*, 2016; Cosme *et al.*, 2017). However, we were able to detect a combination of traits that would prevent wet-habitat species from establishing in dry areas of the Amazon forest. FF and V species had traits associated with fast-resource acquisition but with higher vulnerability of their hydraulic system. Species to establish in P and WS areas need to cope with lower water availability, and water stress may be a key environmental filter limiting the survival of species that can not sustain elevated xylem tensions. In contrast, competition may be the main process impairing the establishment of P and WS species in wet Amazonian environments. Having a slow-resource-acquisition strategy, such as the species found in P and WS areas, is disadvantageous in environments where resources (e.g. water) is constantly available and these species are probably outcompeted by others that are faster in capturing resources (Chapin, 1991; Reich, 2014).

All of the wood, leaf and hydraulic traits we measure showed a non-significant phylogenetic signal (Table S2). This findings suggests that functional traits within wet vs dry environments in the Amazon are more similar than expected, and they evolved repeatedly and independently in close phylogenetic lineages. These patterns can be explained by convergent evolution in functional traits along life-history trade-off axes, in combination with local environmental sorting processes (Fortunel *et al.*, 2013; Gleason *et al.*, 2016; Leibold & Chase, 2017). Moreover, the different environmental conditions found in the Amazon may be a key factor in promoting local speciation by imposing strong environmental pressure in local populations (Leibold & Chase, 2017). This study provides further evidence that tropical tree communities are not randomly assembled. Instead, niche-based processes, such as competition and environmental filtering, are key processes shaping community assemblage in these megadiverse species systems (Baraloto *et al.*, 2012; Fortunel *et al.*, 2013; Cosme *et al.*, 2017; Oliveira *et al.*, 2019).

Much of the variation we found in hydraulic and anatomical traits was related with PCA axis 1, which was also the axis responsible for the clear distinction between wet and dry habitats in the PCA space (Figure 6). These results highlight the importance of hydraulic-related traits in species segregation among the environments and have strong implications for modeling tropical species response to changes in climate. Recently,

newer models such as TFS-Hydro (Christoffersen *et al.*, 2016), Community Land Model version 5 (CLM5), and Ecosystem Demography model 2 (ED2; Xu *et al.*, 2016), have incorporated plant hydraulic traits making substantial improvements in the predictions of vegetation response to changes in temperature and water availability (Anderegg *et al.*, 2016).

To our knowledge, our study is the first to assess plant anatomical (e.g. Dmh and VA) and hydraulic traits (e.g. P_{50}, SM, k_{leaf}, k_h) in the four main habitats of the Amazon Basin. We show for the first time that species from wet and dry environments may be equally vulnerable to future drought events and that water availability can be a robust predictor of species distribution in the Amazonian forests. Although such findings help us understand the processes shaping community assemblages in the tropics and predict the responses of these forests to future drought events, further challenges remain. An exciting and expanding area of study is the role of trait plasticity and acclimation in species survival to a dryer and warmer conditions (e.g. Drake *et al.*, 2018). Also, investigations like the one presented here would benefit by adding similar data and analyses from reciprocal transplant experiments among the contrasting Amazonian habitats to test for local adaptation in tropical tree species' lineages (e.g Fine *et al.*, 2006). Finally, long-term studies that can identify the functional traits and genetic mechanisms that underlie adaptations to distinct climatic regimes will be crucial in understanding species distribution, ecosystem function and climate feedbacks in the future.

Reference

Anderegg WR, Anderegg LD, Berry JA, Field CB. 2014. Loss of whole-tree hydraulic conductance during severe drought and multi-year forest die-off. *Oecologia* 175(1): 11-23.

Anderegg WR, Klein T, Bartlett M, Sack L, Pellegrini AF, Choat B, Jansen S. 2016. Meta-analysis reveals that hydraulic traits explain cross-species patterns of drought-induced tree mortality across the globe. *Proceedings of the National Academy of Sciences* 113(18): 5024-5029.

Andreae M, Acevedo O, Araùjo A, Artaxo P, Barbosa C, Barbosa H, Brito J, Carbone S, Chi X, Cintra B. 2015. The Amazon Tall Tower Observatory (ATTO): overview of pilot measurements on ecosystem ecology, meteorology, trace gases, and aerosols. *Atmospheric Chemistry and Physics* 15(18): 10723-10776.

Baraloto C, Hardy OJ, Paine C, Dexter KG, Cruaud C, Dunning LT, Gonzalez MA, Molino JF, Sabatier D, Savolainen V. 2012. Using functional traits and phylogenetic trees to examine the assembly of tropical tree communities. *Journal of Ecology* 100(3): 690-701.

Baraloto C, Rabaud S, Molto Q, Blanc L, Fortunel C, Herault B, Davila N, Mesones I, Rios M, Valderrama E. 2011. Disentangling stand and environmental correlates of aboveground biomass in Amazonian forests. *Global Change Biology* 17(8): 2677-2688.

Blackman CJ, Gleason SM, Chang Y, Cook AM, Laws C, Westoby M. 2014. Leaf hydraulic vulnerability to drought is linked to site water availability across a broad range of species and climates. *Annals of botany* 114(3): 435-440.

Blomberg SP, Garland Jr T, Ives AR. 2003. Testing for phylogenetic signal in comparative data: behavioral traits are more labile. *Evolution* 57(4): 717-745.

Bonal D, Burban B, Stahl C, Wagner F, Hérault B. 2016. The response of tropical rainforests to drought—lessons from recent research and future prospects. *Annals of Forest Science* 73(1): 27-44.

Brodribb T, Holbrook NM. 2004. Diurnal depression of leaf hydraulic conductance in a tropical tree species. *Plant, Cell & Environment* 27(7): 820-827.

Brum M, Vadeboncoeur MA, Ivanov V, Asbjornsen H, Saleska S, Alves LF, Penha D, Dias JD, Aragão LE, Barros F. 2018. Hydrological niche segregation defines forest structure and drought tolerance strategies in a seasonal Amazon forest. *Journal of Ecology*.

Bucci SJ, Goldstein G, Scholz FG, Meinzer FC 2016. Physiological significance of hydraulic segmentation, nocturnal transpiration and capacitance in tropical trees: Paradigms revisited. *Tropical tree physiology*: Springer, 205-225.

Chapin FS. 1991. Integrated responses of plants to stress. *BioScience* 41(1): 29-36.

Choat B, Jansen S, Brodribb TJ, Cochard H, Delzon S, Bhaskar R, Bucci SJ, Feild TS, Gleason SM, Hacke UG, et al. 2012. Global convergence in the vulnerability of forests to drought. *Nature* 491(7426): 752-755.

Christoffersen BO, Gloor M, Fauset S, Fyllas NM, Galbraith DR, Baker TR, Kruijt B, Rowland L, Fisher RA, Binks OJ. 2016. Linking hydraulic traits to tropical forest function in a size-structured and trait-driven model (TFS v. 1-Hydro). *Geoscientific Model Development* 9(11): 4227.

Connell JH. 1978. Diversity in tropical rain forests and coral reefs. *Science* 199(4335): 1302-1310.

Cosme LH, Schietti J, Costa FR, Oliveira RS. 2017. The importance of hydraulic architecture to the distribution patterns of trees in a central Amazonian forest. *New Phytologist*.

Damasco G, Vicentini A, Castilho CV, Pimentel TP, Nascimento HE. 2013. Disentangling the role of edaphic variability, flooding regime and topography of Amazonian white-sand vegetation. *Journal of Vegetation Science* 24(2): 384-394.

Díaz S, Kattge J, Cornelissen JH, Wright IJ, Lavorel S, Dray S, Reu B, Kleyer M, Wirth C, Prentice IC. 2016. The global spectrum of plant form and function. *Nature* 529(7585): 167.

Doughty CE, Goulden ML. 2008. Are tropical forests near a high temperature threshold? *Journal of Geophysical Research: Biogeosciences* 113(G1).

Drake JE, Tjoelker MG, Vårhammar A, Medlyn BE, Reich PB, Leigh A, Pfautsch S, Blackman CJ, López R, Aspinwall MJ. 2018. Trees tolerate an extreme heatwave via sustained transpirational cooling and increased leaf thermal tolerance. *Global Change Biology* 24(6): 2390-2402.

Engelbrecht BM, Comita LS, Condit R, Kursar TA, Tyree MT, Turner BL, Hubbell SP. 2007. Drought sensitivity shapes species distribution patterns in tropical forests. *Nature* 447(7140): 80-82.

Fan ZX, Zhang SB, Hao GY, Ferry Slik J, Cao KF. 2012. Hydraulic conductivity traits predict growth rates and adult stature of 40 Asian tropical tree species better than wood density. *Journal of Ecology* 100(3): 732-741.

Ferraz J, Ohta S, Sales Pd. 1998. Distribuição dos solos ao longo de dois transectos em floresta primária ao norte de Manaus (AM). *Higuchi, N., Campos, MAA, Sampaio, PTB, and dos Santos, J., Espaço Comunicaçao Ltda., Manaus, Brazil* 264.

Fine PV. 2015. Ecological and evolutionary drivers of geographic variation in species diversity. *Annual Review of Ecology, Evolution, and Systematics* 46: 369-392.

Fine PV, Kembel SW. 2011. Phylogenetic community structure and phylogenetic turnover across space and edaphic gradients in western Amazonian tree communities. *Ecography* 34(4): 552-565.

Fine PV, Miller ZJ, Mesones I, Irazuzta S, Appel HM, Stevens MHH, Sääksjärvi I, Schultz JC, Coley PD. 2006. The growth–defense trade-off and habitat specialization by plants in Amazonian forests. *Ecology* 87(sp7): S150-S162.

Fontes CG, Chambers JQ, Higuchi N. 2018a. Revealing the causes and temporal distribution of tree mortality in Central Amazonia. *Forest Ecology and Management* 424: 177-183.

Fontes CG, Dawson TE, Jardine K, McDowell N, Gimenez BO, Anderegg L, Negrón-Juárez R, Higuchi N, Fine PV, Araújo AC. 2018b. Dry and hot: the hydraulic consequences of a climate change–type drought for Amazonian trees. *Philosophical Transactions of the Royal Society B: Biological Sciences* 373(1760): 20180209.

Fortunel C, Fine PVA, Baraloto C, Dalling J. 2012. Leaf, stem and root tissue strategies across 758 Neotropical tree species. *Functional Ecology* 26(5): 1153-1161.

Fortunel C, Paine CET, Fine PVA, Kraft NJB, Baraloto C, De Deyn G. 2014. Environmental factors predict community functional composition in Amazonian forests. *Journal of Ecology* 102(1): 145-155.

Fortunel C, Ruelle J, Beauchene J, Fine PV, Baraloto C. 2013. Wood specific gravity and anatomy of branches and roots in 113 Amazonian rainforest tree species across environmental gradients. *New Phytol* 202(1): 79-94.

Fu R, Yin L, Li W, Arias PA, Dickinson RE, Huang L, Chakraborty S, Fernandes K, Liebmann B, Fisher R, et al. 2013. Increased dry-season length over southern Amazonia in recent decades and its implication for future climate projection. *Proc Natl Acad Sci U S A* 110(45): 18110-18115.

Gleason SM, Westoby M, Jansen S, Choat B, Hacke UG, Pratt RB, Bhaskar R, Brodribb TJ, Bucci SJ, Cao KF. 2016. Weak tradeoff between xylem safety and xylem-specific hydraulic efficiency across the world's woody plant species. *New Phytologist* 209(1): 123-136.

Grafen A. 1992. The uniqueness of the phylogenetic regression. *Journal of theoretical Biology* 156(4): 405-423.

Hacke UG, Spicer R, Schreiber SG, Plavcová L. 2017. An ecophysiological and developmental perspective on variation in vessel diameter. *Plant, Cell & Environment* 40(6): 831-845.

Jacobsen AL, Pratt RB, Davis SD, Ewers FW. 2007. Cavitation resistance and seasonal hydraulics differ among three arid Californian plant communities. *Plant, Cell & Environment* 30(12): 1599-1609.

Jenkins H, Baker P, Guilderson T 2010. Extreme Drought Events Revealed in Amazon Tree Ring Records. *AGU Fall Meeting Abstracts*.

Kunert N, Aparecido LMT, Wolff S, Higuchi N, dos Santos J, de Araujo AC, Trumbore S. 2017. A revised hydrological model for the Central Amazon: the importance of emergent canopy trees in the forest water budget. *Agricultural and Forest Meteorology* 239: 47-57.

Kunstler G, Falster D, Coomes DA, Hui F, Kooyman RM, Laughlin DC, Poorter L, Vanderwel M, Vieilledent G, Wright SJ. 2016. Plant functional traits have globally consistent effects on competition. *Nature* 529(7585): 204.

Leibold MA, Chase JM. 2017. *Metacommunity ecology*: Princeton University Press.

Marengo JA, Tomasella J, Alves LM, Soares WR, Rodriguez DA. 2011. The drought of 2010 in the context of historical droughts in the Amazon region. *Geophysical Research Letters* 38(12).

McDowell NG. 2011. Mechanisms linking drought, hydraulics, carbon metabolism, and vegetation mortality. *Plant Physiol* 155(3): 1051-1059.

McGill BJ, Enquist BJ, Weiher E, Westoby M. 2006. Rebuilding community ecology from functional traits. *Trends in ecology & evolution* 21(4): 178-185.

Medeiros CD, Scoffoni C, John GP, Bartlett MK, Inman-Narahari F, Ostertag R, Cordell S, Giardina C, Sack L. 2018. An extensive suite of functional traits distinguishes Hawaiian wet and dry forests and enables prediction of species vital rates. *Functional Ecology*.

Medina E, Sobrado M, Herrera R. 1978. Significance of leaf orientation for leaf temperature in an Amazonian sclerophyll vegetation. *Radiation and environmental biophysics* 15(2): 131-140.

Meinzer FC, Johnson DM, Lachenbruch B, McCulloh KA, Woodruff DR. 2009. Xylem hydraulic safety margins in woody plants: coordination of stomatal control of xylem tension with hydraulic capacitance. *Functional Ecology* 23(5): 922-930.

Oliveira RS, Costa FR, van Baalen E, de Jonge A, Bittencourt PR, Almanza Y, Barros FdV, Cordoba EC, Fagundes MV, Garcia S. 2019. Embolism resistance drives the distribution of Amazonian rainforest tree species along hydro-topographic gradients. *New Phytologist* 221(3): 1457-1465.

Pagel M. 1999. Inferring the historical patterns of biological evolution. *Nature* 401(6756): 877.

Pereira L, Bittencourt PR, Oliveira RS, Junior M, Barros FV, Ribeiro RV, Mazzafera P. 2016. Plant pneumatics: stem air flow is related to embolism–new perspectives on methods in plant hydraulics. *New Phytologist* 211(1): 357-370.

Pereira L, Mazzafera P. 2012. A low cost apparatus for measuring the xylem hydraulic conductance in plants. *Bragantia* 71(4): 583-587.

Phillips OL, Vargas PN, Monteagudo AL, Cruz AP, Zans MEC, Sánchez WG, Yli-Halla M, Rose S. 2003. Habitat association among Amazonian tree species: a landscape-scale approach. *Journal of Ecology* 91(5): 757-775.

Poorter L, McDonald I, Alarcon A, Fichtler E, Licona JC, Pena-Claros M, Sterck F, Villegas Z, Sass-Klaassen U. 2010. The importance of wood traits and hydraulic conductance for the performance and life history strategies of 42 rainforest tree species. *New Phytol* 185(2): 481-492.

Powell TL, Wheeler JK, de Oliveira AA, da Costa L, Carlos A, Saleska SR, Meir P, Moorcroft PR. 2017. Differences in xylem and leaf hydraulic traits explain differences in drought tolerance among mature Amazon rainforest trees. *Global Change Biology*.

Reich PB. 2014. The world-wide 'fast-slow' plant economics spectrum: a traits manifesto. *Journal of Ecology* 102(2): 275-301.

Reich PB, Walters MB, Ellsworth DS. 1997. From tropics to tundra: global convergence in plant functioning. *Proceedings of the National Academy of Sciences* 94(25): 13730-13734.

Ribeiro J, Hopkins M, Vicentini A, Sothers C, Costa MdS, Brito Jd, Souza Md, MARTINS L, Lohmann L, Assunção P. 1999. Flora da reserva Ducke: Flora da reserva Ducke: Flora da reserva Ducke: guia de identificação de plantas vasculares de uma floresta de terra-firme na Amazônia Central. *Manaus: INPA*.

Rinne H, Guenther A, Greenberg J, Harley P. 2002. Isoprene and monoterpene fluxes measured above Amazonian rainforest and their dependence on light and temperature. *Atmospheric Environment* 36(14): 2421-2426.

Roberts J, Cabral OM, Costa Jd, McWilliam A, Sá TdA. 1996. An overview of the leaf area index and physiological measurements during ABRACOS. *GASH, JHC; NOBRE, CA; ROBERTS, JM; VICTORIA, RL Amazonian deforestation and climate. Chichester: John Wiley & Sons*.

Saatchi SS, Houghton RA, Dos Santos AlvalÁ RC, Soares JV, Yu Y. 2007. Distribution of aboveground live biomass in the Amazon basin. *Global Change Biology* 13(4): 816-837.

Santiago LS, De Guzman ME, Baraloto C, Vogenberg JE, Brodie M, Hérault B, Fortunel C, Bonal D. 2018. Coordination and trade-offs among hydraulic safety, efficiency and drought avoidance traits in Amazonian rainforest canopy tree species. *New Phytologist*.

Schietti J, Emilio T, Rennó CD, Drucker DP, Costa FR, Nogueira A, Baccaro FB, Figueiredo F, Castilho CV, Kinupp V. 2014. Vertical distance from drainage drives floristic composition changes in an Amazonian rainforest. *Plant Ecology & Diversity* 7(1-2): 241-253.

Scholander PF, Hammel H, Bradstreet ED, Hemmingsen E. 1965. Sap pressure in vascular plants. *Science* 148(3668): 339-346.

Scholz A, Klepsch M, Karimi Z, Jansen S. 2013. How to quantify conduits in wood? *Frontiers in plant science* 4: 56.

Skelton RP, West AG, Dawson TE. 2015. Predicting plant vulnerability to drought in biodiverse regions using functional traits. *Proceedings of the National Academy of Sciences* 112(18): 5744-5749.

Smith TB, Wayne RK, Girman DJ, Bruford MW. 1997. A role for ecotones in generating rainforest biodiversity. *Science* 276(5320): 1855-1857.

Sobrado M. 2009. Leaf tissue water relations and hydraulic properties of sclerophyllous vegetation on white sands of the upper Rio Negro in the Amazon region. *Journal of Tropical Ecology* 25(3): 271-280.

Sperry J, Donnelly J, Tyree M. 1988. A method for measuring hydraulic conductivity and embolism in xylem. *Plant, Cell & Environment* 11(1): 35-40.

Sperry JS. 2004. Coordinating stomatal and xylem functioning–an evolutionary perspective. *New Phytologist* 162(3): 568-570.

Sperry JS, Hacke UG, Pittermann J. 2006. Size and function in conifer tracheids and angiosperm vessels. *American Journal of Botany* 93(10): 1490-1500.

Sperry JS, Meinzer FC, McCULLOH KA. 2008. Safety and efficiency conflicts in hydraulic architecture: scaling from tissues to trees. *Plant, Cell & Environment* 31(5): 632-645.

Stocker TF, Qin D, Plattner G-K, Tignor M, Allen SK, Boschung J, Nauels A, Xia Y, Bex B, Midgley B 2013. IPCC, 2013: climate change 2013: the physical science basis. Contribution of working group I to the fifth assessment report of the intergovernmental panel on climate change: Cambridge University Press.

Stropp J, Van der Sleen P, Assunção PA, da SILVA AL, Ter Steege H. 2011. Tree communities of white-sand and terra-firme forests of the upper Rio Negro. *Acta Amazonica* 41(4).

Stropp J, van der Sleen P, Quesada CA, ter Steege H. 2014. Herbivory and habitat association of tree seedlings in lowland evergreen rainforest on white-sand and terra-firme in the upper Rio Negro. *Plant Ecology & Diversity* 7(1-2): 255-265.

Targhetta N, Kesselmeier J, Wittmann F. 2015. Effects of the hydroedaphic gradient on tree species composition and aboveground wood biomass of oligotrophic forest ecosystems in the central Amazon basin. *Folia Geobotanica* 50(3): 185-205.

Team RC 2014. R: A language and environment for statistical computing. 2014.

ter Steege H, SABATIER D, CASTELLANOS H, VAN ANDEL T, DUIVENVOORDEN J, DE OLIVEIRA AA, EK R, LILWAH R, MAAS P, MORI S. 2000. An analysis of the floristic composition and diversity of Amazonian forests including those of the Guiana Shield. *Journal of Tropical Ecology* 16(6): 801-828.

Tng DY, Apgaua DM, Ishida YF, Mencuccini M, Lloyd J, Laurance WF, Laurance SG. 2018. Rainforest trees respond to drought by modifying their hydraulic architecture. *Ecology and evolution* 8(24): 12479-12491.

Toledo JJ, Castilho CV, Magnusson WE, Nascimento HE. 2017. Soil controls biomass and dynamics of an Amazonian forest through the shifting of species and traits. *Brazilian Journal of Botany* 40(2): 451-461.

Tomasella J, Hodnett MG, Cuartas LA, Nobre AD, Waterloo MJ, Oliveira SM. 2008. The water balance of an Amazonian micro-catchment: the effect of interannual

variability of rainfall on hydrological behaviour. *Hydrological Processes: An International Journal* 22(13): 2133-2147.

Tuomisto H, Ruokolainen K, Yli-Halla M. 2003. Dispersal, environment, and floristic variation of western Amazonian forests. *Science* 299(5604): 241-244.

Valencia R, Foster RB, Villa G, Condit R, Svenning JC, Hernández C, Romoleroux K, Losos E, Magård E, Balslev H. 2004. Tree species distributions and local habitat variation in the Amazon: large forest plot in eastern Ecuador. *Journal of Ecology* 92(2): 214-229.

van Gelder H, Poorter L, Sterck F. 2006. Wood mechanics, allometry, and life-history variation in a tropical rain forest tree community. *New Phytologist* 171(2): 367-378.

Venturas MD, MacKinnon ED, Dario HL, Jacobsen AL, Pratt RB, Davis SD. 2016. Chaparral shrub hydraulic traits, size, and life history types relate to species mortality during California's historic drought of 2014. *PloS one* 11(7): e0159145.

Webb CO, Donoghue MJ. 2005. Phylomatic: tree assembly for applied phylogenetics. *Molecular Ecology Notes* 5(1): 181-183.

Westoby M. 1998. A leaf-height-seed (LHS) plant ecology strategy scheme. *Plant and soil* 199(2): 213-227.

Williamson GB, Wiemann MC. 2010. Measuring wood specific gravity… correctly. *American Journal of Botany* 97(3): 519-524.

Xu X, Medvigy D, Powers JS, Becknell JM, Guan K. 2016. Diversity in plant hydraulic traits explains seasonal and inter-annual variations of vegetation dynamics in seasonally dry tropical forests. *New Phytologist* 212(1): 80-95.

Zanchi FB, Waterloo MJ, Tapia AP, Alvarado Barrientos MS, Bolson MA, Luizão FJ, Manzi AO, Dolman AJ. 2015. Water balance, nutrient and carbon export from a heath forest catchment in central Amazonia, Brazil. *Hydrological Processes* 29(17): 3633-3648.

Zanne AE, Westoby M, Falster DS, Ackerly DD, Loarie SR, Arnold SE, Coomes DA. 2010. Angiosperm wood structure: global patterns in vessel anatomy and their relation to wood density and potential conductivity. *American Journal of Botany* 97(2): 207-215.

Zuleta D, Duque A, Cardenas D, Muller-Landau HC, Davies S. 2017. Drought-induced mortality patterns and rapid biomass recovery in a terra firme forest in the Colombian Amazon. *Ecology*.

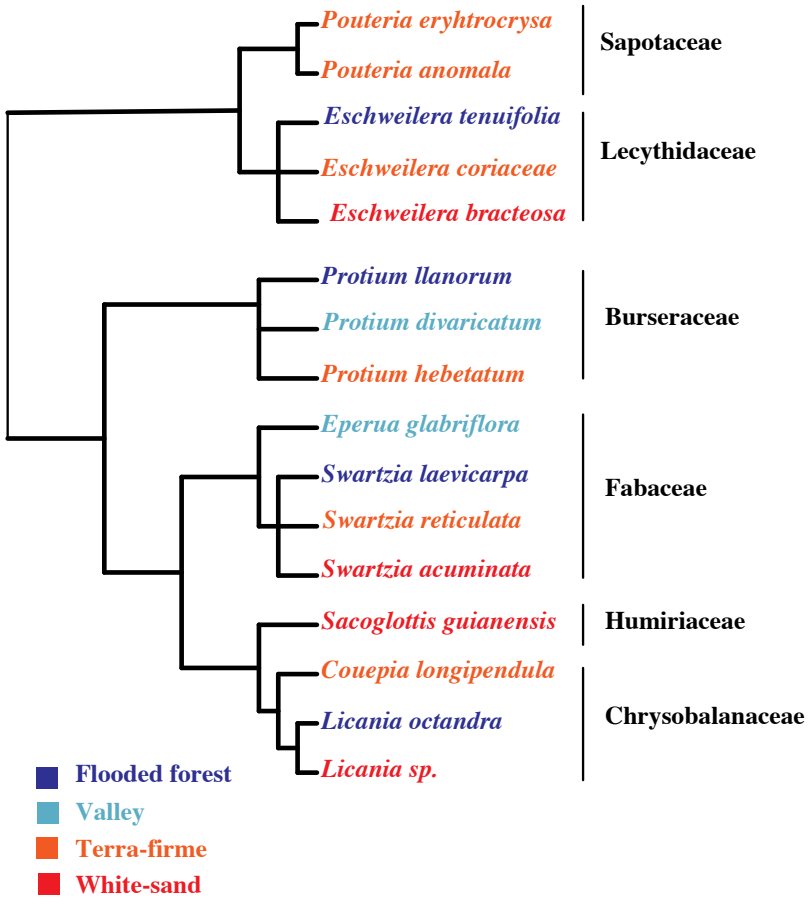

Figure 1. The evolutionary relationship of 16 tropical tree species selected for this study. The cladogram is based on the maximum resolved angiosperm phylogeny (APG III R20120829). Colors indicate the four different environments the species are mainly found.

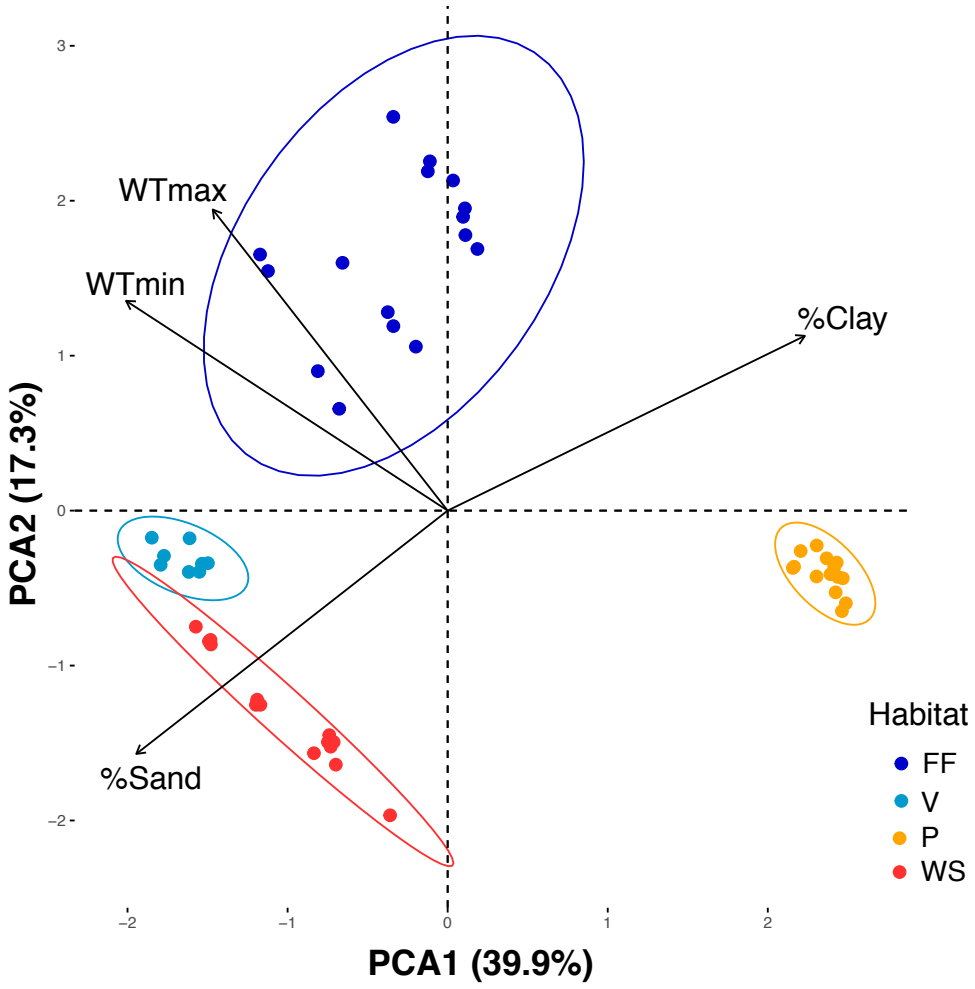

Figure 2. Principal components analysis (PCA) on soil texture (%Clay and %Sand) and minimum and maximum water table depth (WTmin and WTmax respectively) across the network of 52 forest plots. The first two axes of the PCA account for 96.8% of the total variation among the plots where individuals were sampled. The different colors represent the habitat the individuals were collected from. FF = flooded forest, P =plateau forest, V = valley forest and WS = white-sand forest.

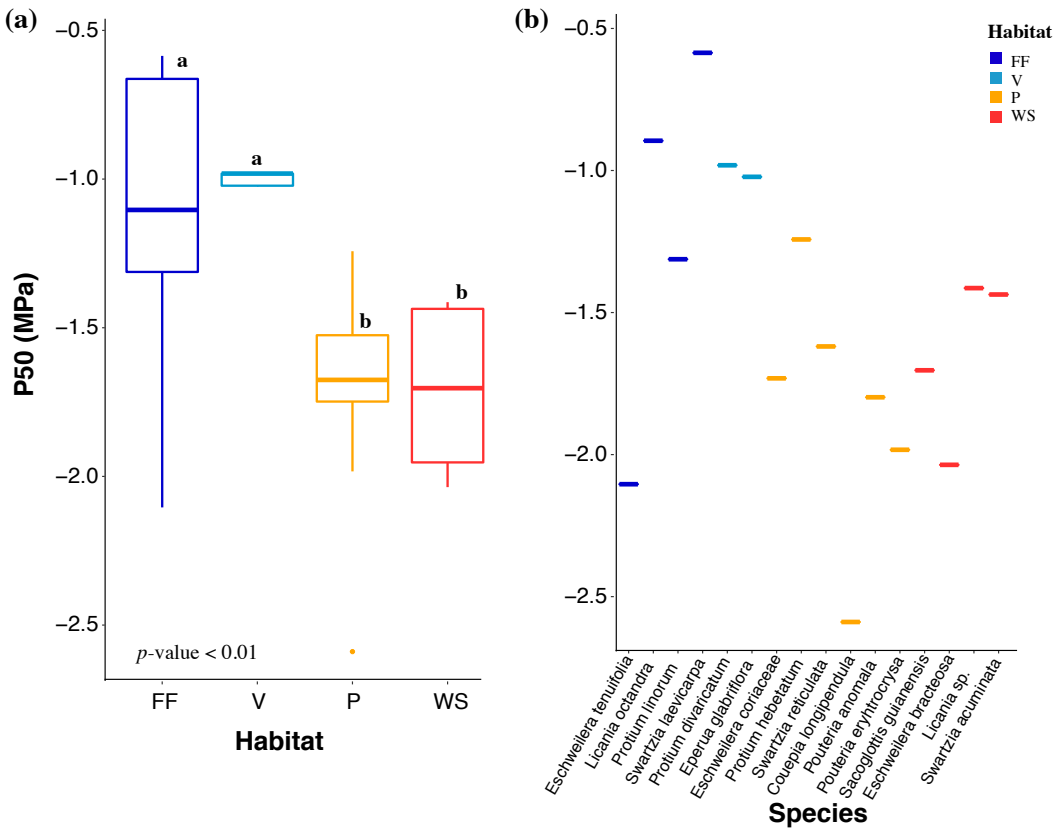

Figure 3. (a) Boxplot of water potential at 50% loss of xylem hydraulic conductivity (P50) among the different habitats. The lines in the box indicate the mean, and the lines above and below the box indicate the maximum and minimum values respectively. **(b)** P50 values of the 16 studied species. Tukey's HSD test is indicated in bold letters, with significance of 0.01 (ANOVA *p*-value = 0.010). Colors represent the four habitats, flooded forest (FF): dark blue, valley (V): light blue, plateau (P): yellow and white-sand (WS): red.

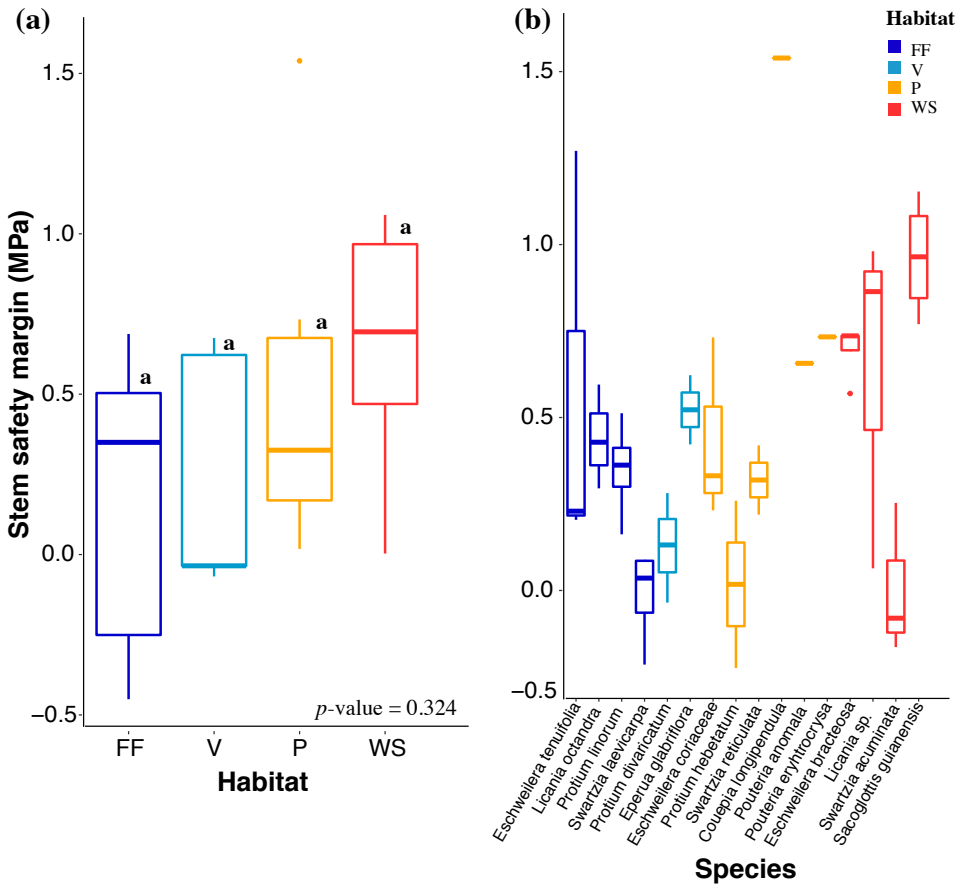

Figure 4. (a) Boxplot of stem hydraulic safety margin (SM = P_{min} - P_{50}) among the different habitats. The lines in the box indicate the mean, and the lines above and below the box indicate the maximum and minimum values respectively. **(b)** SMs of the 16 studied species. SMs among the four environments were not significantly different (ANOVA *p*-value = 0.324). Colors represent the four habitats, flooded forest (FF): dark blue, valley (V): light blue, plateau (P): yellow and white-sand (WS): red.

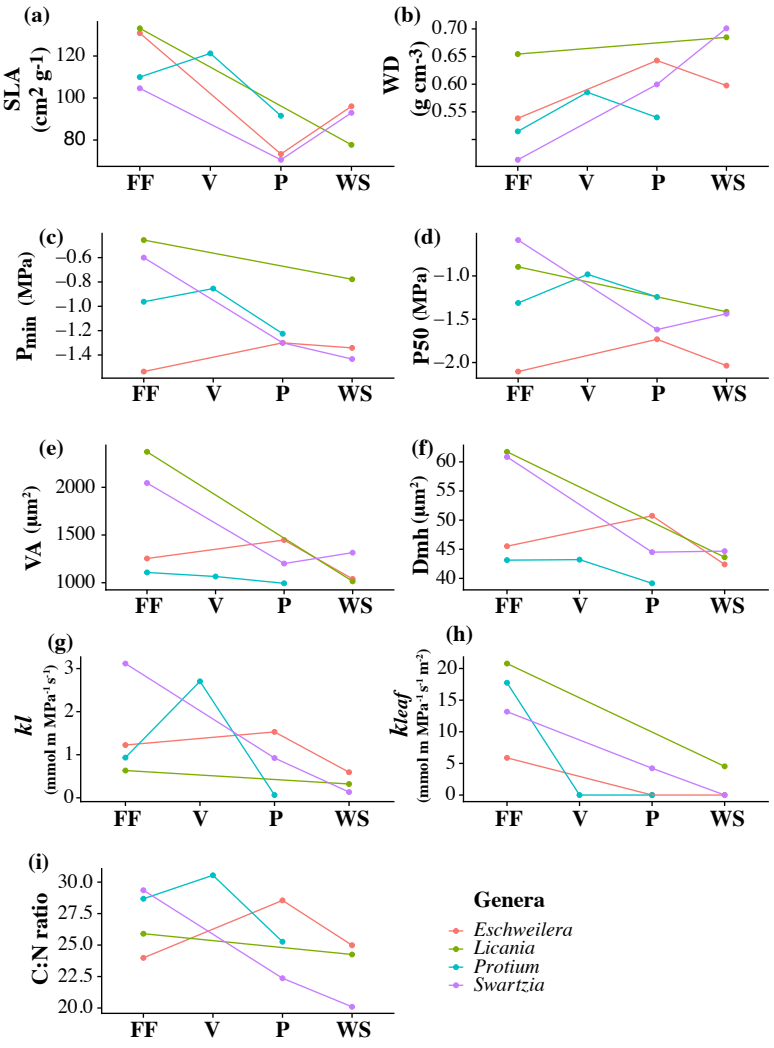

Figure 5. (a) Specific leaf area, **(b)** wood specific gravity , **(c)** midday leaf water potential, **(d)** water potential at 50% loss of hydraulic conductivity, **(e)** mean vessel area, **(f)** mean vessel hydraulic diameter, **(g)** stem conductance, **(h)** leaf specific hydraulic conductivity, **(i)** C:N ratio, for 3 triplets (*Eschweilera, Protium,* and *Swartzia*) and 1 pair (*Licania*) of congeneric species associated with four contrasting environments (FF: flooded forest, V: valley, P: Plateau and WS: white-sand forest). Lines connect congeneric species occuring in different environments, and values of significance (*p*-value) for the ANOVA test are shown for each trait. According with the Tukey HSD test, for all traits, there was no significant difference between the two wet (FF and V) or the two dry (P and WS). All relationships are shown in original measurement units, but for the ANOVA and Tukey HSD tests we used log-transformed values of number of stomata, k_{leaf}, k_h, C:N ratio, vessel fraction, vessel size to number ratio, mean xylem hydraulic diameter and mean vessel area to achieve normality. The different colors indicate the four phylogenetic lineages (red: Lecythidaceae, green: Chrysobalanaceae, blue: Burseraceae, purple: Fabaceae) sampled.

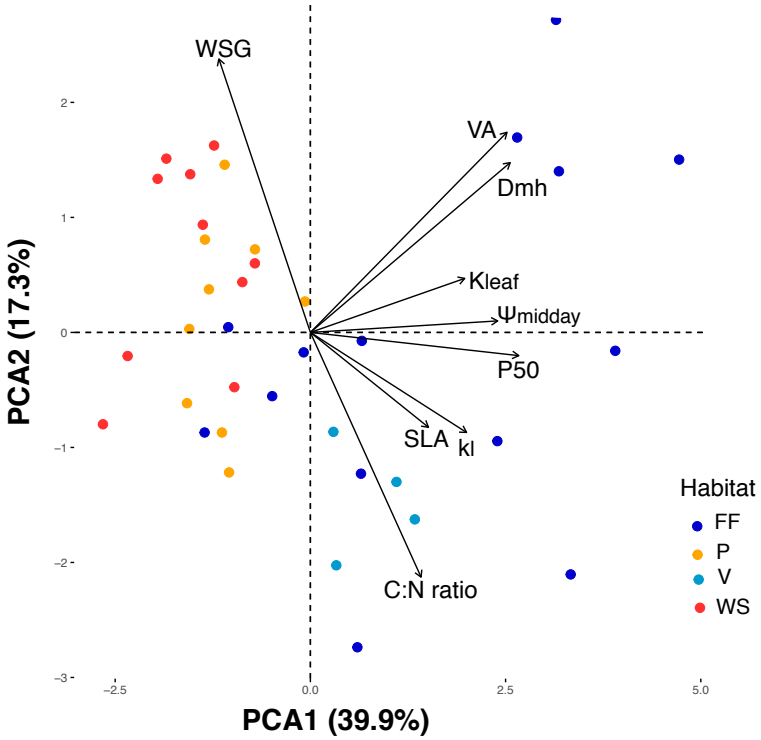

Figure 6. Principal components analysis (PCA) of the 37 individuals, belonging to 11 tree species. Colors represent the four habitats, flooded forest (FF): dark blue, valley (V): light blue, plateau (P): yellow and white-sand (WS): red. The 9 significant traits from Fig.5 were included: WSG = wood specific gravity (g cm^{-3}), VA = mean vessel area (μm^2), Dmh = mean vessel hydraulic diameter (µm), k_{leaf} = leaf hydraulic conductivity (mmol m MPa^{-1} s^{-1} m^{-2}), Ψ_{midday} = midday water potential (MPa), P50 = water potential when 50% of xylem conductivity is lost (MPa), *kl* = stem hydraulic conductance (mmol m MPa^{-1} s^{-1}), SLA = specific leaf area (cm^2 g^{-1}), and C:N ratio (%).

CHAPTER 2 Dry and hot: the hydraulic consequences of a climate change–type drought for Amazonian trees

Abstract

How plants respond physiologically to leaf warming and low water availability may determine how they will perform under future climate change. In 2015-2016 an unprecedented drought occurred across Amazonia with record-breaking high temperatures and low soil moisture, offering a unique opportunity to evaluate the performances of Amazonian trees to a severe climatic event. We quantified the responses of leaf water potential, sap velocity, whole-tree hydraulic conductance (K_{wt}), turgor loss and xylem embolism, during and after the 2015-2016 El Niño for five canopy-tree species. Leaf/xylem safety margins (SM), sap velocity and K_{wt} showed a sharp drop during warm periods. SMs were negatively correlated with vapor pressure deficit but had no significant relationship with soil water storage. Based on our calculations of canopy stomatal and xylem resistances, the decrease in sap velocity and K_{wt} was due to a combination of xylem cavitation, and stomatal closure. Our results suggest extremely warm droughts greatly amplify the degree of trees' physiological stress and can lead to mortality. Given the extreme nature of the 2015-2016 El Niño and that temperatures are predicted to increase, this work can serve as a case study of the possible impact climate warming can have on tropical trees.

Introduction

The paleoecological records show that the Amazon basin has experienced droughts in the past (Irion *et al.*, 2006; Mayle & Power, 2008; Marengo & Espinoza, 2015), however the frequency, duration, and intensity of these climatic events have recently accelerated, imposing a novel and significant challenge for plant communities (Jenkins *et al.*, 2010; Stocker *et al.*, 2013; Doughty *et al.*, 2015). Currently, there is a lack of *in situ* data on how the combination of high leaf temperature and low soil water may impact the way plants regulate their water consumption in the tropics. In 2015-2016 a strong El Niño occurred, with record-breaking high temperatures and low precipitation (Jiménez-Muñoz *et al.*, 2016), offering a unique opportunity to evaluate how Amazonian trees in their natural environment respond physiologically to severe changes in water supply and demand.

Future droughts are projected to become increasingly severe due to warming (Trenberth *et al.*, 2014). Air warming intensifies tree stress by driving a non-linear increase in vapor pressure deficit (VPD), causing greater water loss through plant stomata and from the soil surface (Jung *et al.*, 2010; Eamus *et al.*, 2013; Allen *et al.*, 2015). Moreover, canopy leaves in tropical forests are usually warmer than air temperature, and an increase of 3ºC in air temperature can elevate VPD by 45% (Will *et al.*, 2013). Studies show that leaf photosynthesis and stomatal conductance decline at leaf temperatures

above the optimal value of around 30-35ºC (Doughty & Goulden, 2008; Doughty *et al.*, 2015), and trees are also at a greater risk of losing water transport capacity or suffering hydraulic failure during hot droughts (McDowell *et al.*, 2008; Anderegg *et al.*, 2013; Anderegg *et al.*, 2014). Because wet tropical ecosystems are thermally stable, many tropical plants may lack the ability to avoid highly negative xylem pressure caused by extreme climate warming (Janzen, 1967; Doughty & Goulden, 2008; Gleason *et al.*, 2016).

Plant hydraulic characteristics are thought to play a critical role in survival during drought (e.g. Bartlett *et al.*, 2012; Oliveira, 2013; Powell *et al.*, 2017). Traits commonly used as indicators of plant water stress tolerance are the leaf water potential at the turgor loss point (Ψ_{tlp}), and stem xylem vulnerability to cavitation (Tyree & Sperry, 1989; Maréchaux *et al.*, 2015; Binks *et al.*, 2016). These two traits represent live (leaf cells) and dead (xylem) tissues that play key roles in plant performance and survival. Oddly, few studies on tropical trees have measured both of these traits and therefore may give us an incomplete picture of a plant's resistance, tolerance and overall response to high temperature and water deficit.

Leaf turgor loss (π_{tlp}) or leaf wilting point, is a useful metric to quantify leaf and plant drought tolerance and is usually calculated using leaf Pressure-Volume (PV) curves (Binks *et al.*, 2016; Williams *et al.*, 2017). A more negative π_{tlp} enables a plant to acquire water from drier soils and to maintain leaf function at lower leaf water potentials (Bartlett *et al.*, 2012; Binks *et al.*, 2016). Similarly, plants' ability to resist xylem cavitation at high xylem tension is advantageous because it allows them to transport water and fix CO_2 under drier conditions (Tyree & Sperry, 1989). The most commonly used indexes of xylem embolism resistance are Ψ_{50} and $\Psi_{88,}$ quantified as the value of xylem water potential (Ψ_x) causing 50% or 88% loss of xylem hydraulic conductivity (e.g. Choat *et al.*, 2012; Trifilò *et al.*, 2015; Powell *et al.*, 2017). These leaf and xylem metrics (π_{tlp}, $\Psi_{50,}$ and Ψ_{88}) can then be used to calculate hydraulic safety margins (Delzon & Cochard, 2014).

Here we present two-years of leaf and xylem physiological measurements, along with climatic data to investigate how the combination of high atmospheric water demand and low water supply, imposed by the 2015-2016 El Niño, impacted the performance of five different Amazonian tree species. We present local climatic and environmental data to characterize the soil water deficit (supply) and the increase in vapor pressure deficit (VPD; demand) during the 2015-2016 drought. Then we test the following hypotheses: (1) species' leaf, and xylem hydraulic safety margins (SM) will narrow with an increase in VPD or decrease in soil water supply; (2) the decline in sap velocity during the drought will be mainly explained by a decrease in whole-tree hydraulic conductance caused by increased xylem resistance due to a spread in xylem embolism.

Materials and Methods

Study site

The study was conducted at the 55m K34 tower (2°35.37′S, 60°06.92′W), situated 3km away from the main dirt road in the Reserva Biológica do Cueiras and located 90km north-northwest of the city of Manaus, Brazil (Araújo *et al.*, 2002). The site (known as ZF-2) is administered by INPA (Instituto Nacional de Pesquisas da Amazônia) under the

Large-Scale Biosphere–Atmosphere Experiment in Amazonia (LBA) program. The mean monthly temperature is 26°C, and annual rainfall is around 2000 to 2600 mm, with a dry season between July and September (Sombroek, 2001; Higuchi *et al.*, 2011). The vegetation in this area is old-growth, *terra-firme* rainforest, with a leaf area index of 5–6 and an average canopy height of 30 m. The soil on this medium-size plateau area is mainly Oxisols with high clay content (Luizão *et al.*, 2004).

Plant measurements and experimental protocols

Leaf water potential, sap velocity and pressure-volume measurements were sampled from five tree species (one individual per species) around K34 tower. *Pouteria anomala* ((Pires) T.D.Penn.) (Sapotaceae) 35.3cm in diameter at breast height (DBH, 1.3m) and 31m in height, *Pouteria erythrochrysa* (T.D.Penn) (Sapotaceae) with 36.5cm DBH and 29.3m in height, *Eschweilera cyathiformis* (S.A.Mori) (Lecythidaceae) with 14.3cm of DBH and 19.8m height, *Couepia longipendula* (Pilg.) (Chrysobalanaceae) with 28.1cm of DBH and 23.9m in height, and *Eschweilera* sp. (Mart. ex DC.) with 29.7cm of DBH and 27.8m in height. These three genera encompass ~25% of all individuals found in the area (based on unpublished studies in permanent plots located ~2km from the study site) and are good representatives of the overall community. Four of the trees were upper canopy with direct sunlight exposure; *E. cyathiformis* was a mid canopy tree that receives mostly indirect sunlight. For plant hydraulic measurements an additional 12 individuals, 16 individuals at total (3-5 per species), were sampled as described below.

Leaf water potential: Leaf water potential (Ψ_{leaf}) was measured using a Scholander pressure chamber (PMS, Corvallis, OR, USA; accurate to 0.05 MPa; Scholander *et al.*, 1965). One sun leaf per study tree was collected hourly from 6:00 to 18:00 and Ψ_{leaf} measurements were made as soon as the leaf was cut from the branch. The leaves were always collected from the same height (20m ± 5m). The Ψ_{leaf} measurements were carried out once a month from July 2015 to July 2017, characterizing the Ψ_{leaf} variation during and after the 2015-2016 El Niño.

Pressure-volume curves: the measurements were carried out from November to December 2015. Three small branches (~ 1 m length) from each studied tree were harvested in the late afternoon, submerged in tap water and placed in a dark room to encourage overnight hydration. Pressure-volume (PV) curves of ten leaves per tree species were generated the next morning using bench drying and repeat pressurization methods (Tyree & Hammel, 1972; Hinckley *et al.*, 1980; Sack *et al.*, 2003). As the leaves dried out, together with $\Psi_{leaf,}$ leaf mass was determined from the average of three leaves with precision of +/- 0.1mg. Complete leaf PV curves were generated after 3-8 hours of dehydration period. Dry mass was determined after 72h at 70°C. Points on the PV curve that were indicative of over hydration (so-called 'plateau effects') were identified and corrected as suggested by Kubiske and Abrams (1991). Species turgor loss point (π_{tlp}) was calculated using the measured PV curves as described in Koide et al. (Koide *et al.*, 1989) . Although π_{tlp} has been shown to vary through time, our sampling was at the peak of the drought. Therefore the π_{tlp} measured in this study likely represents the extreme negative π_{tlp} these species manifest.

Xylem vulnerability curves: we assessed species' xylem vulnerability to cavitation and generated xylem vulnerability curves for four of the focal species (*P. anomala, P. erythrochrysa*, *E. cyathiformis* and *C. longipendula*). In addition, we sampled 2-4 additional individuals per species (a total of 3 to 5 individuals/species) found in nearby plots. These additional trees appeared visibly healthy, had similar diameters (± 5 cm in DBH) and canopy positions as the focal tree species near K34 tower and all branches were collected from ~20-25m height. Maximum vessel lengths were estimated from the mean maximum vessel length measured (varied from 10.5 to 48.5 cm) on a minimum of 3 individuals per species (Jacobsen *et al.*, 2007b). Xylem vulnerability to cavitation was then measured using the bench dehydration method (Sperry *et al.*, 1988) using an ultra-low-flow meter (Pereira & Mazzafera, 2012; Pereira *et al.*, 2016). The xylem pressures when 50% of conductivity is lost (Ψ_{50}), and when 88% of conductivity is lost (Ψ_{88}) for each species were then determined using the fatigue-corrected PLC curves (Hacke *et al.*, 2001; Jacobsen *et al.*, 2007a; Paddock III *et al.*, 2013). We followed the protocols of Pereira and Mazzafera (2012) to assemble the hydraulic apparatus and determine the vulnerability curve. For more details on how the PLC curves were generated please refer to the SI (Methods S1).

Leaf and xylem safety margins**:** Leaf safety margin (SM_{leaf}) was calculated as $SM_{leaf} = \Psi_{min} - \Psi_{TLP}$; where Ψ_{min} is the minimum leaf water potential measured in a particular day, and Ψ_{TLP} is the leaf water potential at turgor loss point (calculated using pressure-volume curves). Xylem safety margins ($SM_{P50,}$ and SM_{P88}) were calculated as $SM_{P50} = \Psi_{min} - \Psi_{P50}$ and $SM_{P88} = \Psi_{min} - \Psi_{P88}$; where Ψ_{P50} and Ψ_{P88} are, respectively, when 50 or 88% of the xylem hydraulic conductivity is lost.

Sap velocity and whole-tree hydraulic conductance**:** Sap velocity measurements started in March of 2015 before the 2015-2016 drought hit Central Amazon. We installed one heat ratio sap flow sensor (Green *et al.*, 2003; SFM1, ICT international) per focal tree at breast height with a 5 min measurement cycle. Throughout the experiment, we moved (~2) the sensors to different locations on the stem. Tree biophysical characteristics for each tree, together with Sap Flow Tool version 1.4.1 (ICT International/Phyto-IT) were used to calculate sap velocities from raw data downloaded from the SFM1 sap flow sensors in the field. Sap velocity was measured from March of 2015 to February 2017 for the species *P. anomala*, *P. erythrochrysa*, *E. cyathiformis* and *Eschweilera* sp.. Due to field logistics and sensor availability, the sap flow measurements for *C. longipendula* were discontinued in mid-September 2015.

According to Darcy's Law, $\Delta\Psi_{leaf}$ ($\Delta\Psi_{leaf} = \Psi_{midday} - \Psi_{predawn}$) and normalized sap velocity data (Q; Gorla *et al.*, 2015) were used to estimate whole-tree hydraulic conductance (K_{wt}) as follows (for details see SI Methods S2):

$$Kwt = \frac{Q}{\Delta\Psi leaf} \qquad \text{(Equation 1)}$$

To investigate the mechanism behind the decrease of K_{wt} and sap velocity during the drought we calculated xylem resistance and canopy stomatal resistance. Normalized xylem resistance ($1/K_s$) was determined using percent loss of conductivity from minimum water potential measurements and xylem vulnerability curves as follows: $K_{s[i]} = 100\text{-}PLC_{i,}$ where PLC_i is the percent loss of conductivity at water potential *i*. The normalized value of K_s was obtained by dividing $K_{s[i]}$ to $K_{s[max]}$.

The canopy stomatal resistance was calculated using Fick's law, RH, T_{air} and T_{leaf} as follows (Murray, 1966; Ewers & Oren, 2000):

$$Gs = \frac{E}{\Delta VPD} \quad \text{(Equation 2)}$$

$$\Delta VPD = (ei * RHi) - (eo * RHo) \quad \text{(Equation 3)}$$

$$e = 0.611 * 10^{7.5*\frac{T}{237.7+T}} \quad \text{(Equation 4)}$$

Where E is the transpiration rate, which in steady state is equal to sap flow (Q) and ΔVPD is the vapor pressure difference in kPa between leaf substomatal chamber (e_i * RH_i) and atmosphere (e_o * RH_o). RH_i and RH_o are relative humidity, expressed as a decimal, inside (we assumed is equal to 1) and outside (air) the leaf, respectively. e_i and e_o are saturated vapor pressure in kPa inside and outside the leaf, respectively. Finally, T is either equal to canopy/leaf temperature (to calculate e_i) or air temperature (when calculating e_o) and is expressed in degrees Celsius.

Environmental variables

Vapor pressure deficit (VPD)**:** A set of thermohygrometers (HC2S3, Campbell Scientific, Logan, UT, USA) were deployed at several heights along the K34 tower, above and beneath the canopy (Araújo *et al.*, 2002). Air relative humidity and temperature, used to calculate VPD, at 28 - 35m height were measured every 60 seconds and recorded as 30 min averages. Computation of VPD was performed following the Clausius-Clapeyron equation. This dataset was provided by the LBA experiment. Thirty minutes averages of VPD were used in all the analyses.

Leaf, canopy and air temperature**:** Leaf temperature was assessed at the peak of the El Niño (September 2015) with a NIST calibrated thermal imaging camera (FLIR-E5, Omega Engineering, 160 x 120 IR resolution; 2% accuracy). Photos were taken hourly (6:00-18:00) at a distance of 1m just prior to leaf removal for Ψ_{leaf}. To measure canopy surface temperature (T_{canopy}), five infrared radiometer sensors (SI-111 and SI-131, Apogee) with an ultra-narrow field of view (14° half-angle; approximate view area of 0.2 m^2) were installed ~20cm from the target branch on the K34 tower at 21.8, 22.8, 24.0, 25.3, and 28.8m height. Five-minute averages of crown temperature were recorded on a data logger (CR-3000 Campbell Scientific® for the SI-111 analogical sensors and EM-50 Decagon® for the SI-131 digital sensors). Five minute average data was used for all the analysis. In addition we used the AIRS (Atmospheric Infrared Sounder 1º of resolution) surface air temperature data (AIRS3STM V6, available at giovanni.gsfs.nasa.gov) centered on the Amazon field site to assess long-term series of surface air temperature before, during and after the 2015-2016 El Niño.

Precipitation, soil moisture and water table depth**:** monthly rainfall data, from 2002-2016, was provided by the LBA hydrology group. Most of the data used in this study come from the T7 pluviometer, located at the K34 tower. When data from T7 was not available, data from the S1 pluviometer located ~3 Km away from the K34 tower was used. The LBA hydrology group also contributed with monthly soil moisture (~150m from the K34 tower) and water table depth (~500m from the K34) data from January-

2014 to April-2016 (SI Table S1). This dataset has soil moisture information until 300 cm depth. However, the days/times of data collection did not overlap with the water potential measurements. Therefore, we were not able to run time-stamp analyses with this dataset and we only used it to characterize the fluctuations of volumetric soil water in the first 300 cm of the soil during the drought event. To perform coordinated and time-stamp analyses, we had an additional dataset where daily volumetric soil water content (VWC) was measured every 30 min, from September 2015 to July 2017. These measurements were performed with a Water Content Reflectometer (CS655 Campbell Scientific, Logan, UT, USA) located ~12m from the K34 tower. VWC was measured at five soil's depths: 10, 20, 40, 60 and 100 cm. Soil water storage (SWS in cm) in the first 100 cm of the soil was calculated using the formula:

$$SWS = \sum_{i=1}^{n} \theta i, t \ * \ \Delta Z \qquad \text{(Equation 5)}$$

Where n is the number of layers in the soil profile, $\theta_{i,t}$ is the volumetric water content in layer i at time t, and ΔZ is the depth increment from layer i to i+1.

Statistical analyses

We used linear mixed-effect models (individual trees as random effects) to evaluate the relationship between VPD, canopy temperature, and SWS and plant's safety margins. For these analyses we tested four models, Model 1: all species share the same slope and intercept; Model 2: the species have different intercepts but the same slope; Model 3: species have different slopes but the same intercept; and Model 4: species can have different intercepts and slopes. We report the results of the models with the lowest AIC value. To test which environmental variable, VPD or SWS, best explained species' safety margin values, we compared three models, Model VPD: VPD as the only independent variable, Model SWS: SWS as the only independent variable and Model VPD + SWS: VPD and SWS as the independent variables. Analysis of covariance (ANCOVA) with a random species effect was used to assess the relationship between sap velocity before and during the 2015-2016 El Niño and VPD, and between sap velocity and SWS during and after the drought. All models were implemented in R v.3.0.2 (R Development Core Team, 2013).

Results

Record-breaking high temperatures and high vapor pressure deficits were observed during the 2015-2016 drought

During previous droughts (e.g. 2009-2010) high temperatures or low precipitation were observed (Fig.1). However, during the 2015-2016 El Niño, higher temperatures (2% or 1.2ºC higher) and lower precipitation (~25% or 31 mm lower) for the months of August-December, compared to the long-term average were recorded (Fig. 1a). In

particular, a 20% (22.8 mm) reduction in precipitation was observed during August-December of 2015 relative to the same period in 2010 (SI Fig.S1), thus 2015 may be the hottest year in Amazonia in the last 100-years (Jiménez-Muñoz *et al.*, 2016).

The record low in precipitation during the 2015-2016 El Niño contributed to ~8% (0.2 cm^3 cm^3) and 11% (2.12 m) lower volumetric soil water content and water table depth, respectively, in relation to the dry season of 2014 (Fig. 1b). However, the absolute changes in soil water content in the first 3m of the soil were small, suggesting water supply for plants were not very limited during the study period.

Satellite observations revealed that September 2015 exhibited the warmest monthly averaged surface air temperature of any other month over the past 13 years at the study site (Fig. 2b). Daytime air temperatures in September were nearly 1.0 ºC warmer than any month from other dry years (2005 and 2010). A maximum daytime canopy temperature of upper canopy leaves increased 5-7ºC during the drought compared to the pre-drought period (Fig. 2a). Furthermore, during the peak of the El Niño (September/2015), individual sun-exposed leaf temperatures of the study trees reached ~ 47ºC ± 1ºC, almost 10ºC higher than the maximum canopy temperature registered in that month (Fig 2a,c). Due to an increase in air temperature and a decrease in air relative humidity, VPD also increased in the El Niño months (Fig. 2a), reaching ~5 kPa during the day and 1 kPa during the night (in September 2015), 40% and 95% higher respectively, then after the drought (Fig. 2a).

H1: Species' leaf, and xylem hydraulic safety margins will narrow with an increase in vapor pressure deficit or decrease in soil water supply

We analyzed leaf and xylem safety margins (SM_{leaf} and $SM_{P50,88}$ respectively) during and after the 2015-2016 El Niño to determine the sensitivity of plants to vapor pressure deficit (VPD) and soil water storage (SWS). Daily minimum leaf water potential (Ψ_{min}) measurements throughout the drought (August to December 2015) were significantly different (paired-sample t-test: p-value = 7.179 e^{-5}) and up to 1.9 MPa (59%) more negative than during the same period in 2016 (Fig. 3). Even though we found a high variation in species response to the drought (Fig. 3 and SI Fig. S2) plant's SMs, regardless of species, were highly sensitive to changes in VPD (Fig. 4) and T_{Canopy} (SI Fig. S3). An increase of 1 kPa in VPD caused a decrease of 0.43 and 0.34 MPa in SM_{leaf} and SM_{P50}, respectively (SI Table. S2). Applying a more conservative xylem safety margin (SM_{P88}) showed a similar relationship between SM and VPD (Fig. 4c).

On the other hand, the relationship between SM_{leaf}, SM_{P88} and SWS was non-significant (p-value = 0.842 and 0.171 respectively). The relationship between SM_{P50} and SWS was weak (estimate = -0.13 and p-value = 0.0378) and species had statistically similar slopes but random intercepts (SI Table S3). In addition, when comparing the models used to test the effect of VPD, SWS and VPD + SWS on trees' SMs, only Model VPD was statistically significant (p-value = 0.005; SI Table S4). Furthermore, predawn measurements during the drought were high (~0.3 MPa; Fig. 3) and had a weak relationship with SWS (SI Fig. S4 and Table S5), suggesting that soil water availability was not limiting during our study period. These results indicate that atmospheric demand

but not soil water supply was driving the decrease in plants' SMs observed during our study period.

H2: The decline in sap velocity during the drought will be mainly explained by a decrease in whole-tree hydraulic conductance caused by increased xylem resistance due to a spread in xylem embolism.

Sap velocity and whole-tree hydraulic conductance (K_{wt}) during the peak of the 2015-2016 drought had a ~35 and ~70% reduction, respectively, compared to values recorded before and after the El Niño (Fig. 5). The decline in sap velocity was correlated with an increase in VPD, but had a weak correlation with soil water storage (Fig 6a and b; SI Table S6), corroborating our findings that atmospheric demand had a greater impact on plant's physiological performance than water supply during our study period. Furthermore, species that substantially crossed their P_{50} during the El Niño (e.g. *E. cyathiformis*) were not able to completely recover sap velocity to pre-drought values (Fig. 3 and 5), indicating that the drought caused permanent damage to species' xylem. Finally, based on our calculations of canopy stomatal ($1/G_s$) and xylem ($1/K_s$) resistances, the decrease in sap velocity and K_{wt} was due to a combination of xylem cavitation, and stomatal closure (Fig. 7a-c). Therefore, we reject our hypothesis that the decrease in sap velocity and K_{wt} was mainly explained by an increase in xylem cavitation.

Discussion

This study reveals how leaf water relations and xylem transport characteristics in five Amazonian trees species, responded to a severe hot and dry climate event, and whether these responses were related to an increase in VPD, a decrease in SWS and xylem embolism formation. The studied trees showed great sensitivity to unusually high canopy temperatures and VPD but not to superficial soil water content. Moreover, during the El Niño, due to a high atmospheric demand, tree transpiration declined. Finally, despite the stomatal closure, the studied trees showed increased xylem embolism that affected their ability to transport water to tree crowns under the warmer and drier El Niño conditions.

Effects of the 2015-2016 drought on local climatic variables

The precipitation and soil water data in the central Amazon (Fig. 1) indicate that the 2015-2016 El Niño was the most severe drought seen in the last decade, surpassing the so-called 'once in a century' droughts of 2005 and 2010 (Lewis *et al.*, 2011; Marengo *et al.*, 2011; Jiménez-Muñoz *et al.*, 2016). Along with the very low water supply, the atmospheric demand for water from the forests also increased (Fig. 2). The long-term air temperature data corroborate the findings that 2015-2016 El Niño contributed to the hottest year in the last decade (Jiménez-Muñoz *et al.*, 2016). Leaf temperatures were also record-breaking, reaching values (~ 47^{o}C; Fig 2) that have been shown to denature leaf proteins such as Rubisco and cause oxidative damage to photosynthetic structures (Salvucci *et al.*, 2001). VPD was also considerably higher (~40-95%) during the drought than after the El Niño (Fig. 2), exacerbating physiological stress on plants by increasing plant water loss and reducing net carbon uptake (McDowell *et al.*, 2008). Our results,

showing the physiological responses of five Amazonian trees to this novel and extremely hot and dry conditions, provides an important example of how trees may be impacted by future climatic events.

H1: Species' leaf, and xylem hydraulic safety margins will narrow with an increase in vapor pressure deficit or decrease soil water supply

A significantly negative relationship between leaf (SM_{leaf}) and xylem (SM_{P50} and SM_{P88}) safety margins and VPD was found (Fig. 4), indicating that plants' live and dead tissues are both sensitive to an increase in temperature and VPD. In addition, the high temperatures recorded during the drought, coupled with low air relative humidity, caused most species to operate under negative safety margins (SM_{leaf} and SM_{P50}). These results suggest that future extreme warming events can be particularly stressful for some Amazonian trees, and corroborate findings that warmer temperatures greatly amplify tree's stress and potentially mortality (Doughty & Goulden, 2008; Trenberth *et al.*, 2014; Allen *et al.*, 2015; Doughty *et al.*, 2015).

Interestingly, the predawn leaf water potential ($\Psi_{predawn}$) values were high (Fig. 3), suggesting that soil water availability was never limiting during our study period. This interpretation is consistent with the small absolute changes in soil water content (Fig. 1b) in the first 300 cm of the soil, and with the weak relationship found between SM_{P50} and SWS (Fig. 4 d-f) and sap velocity and SWS in the first 100 cm of the soil (Fig. 6b). As concluded by a previous study at the same site, more than 40% of the total demand for transpiration is supplied by the first 100 cm of the soil, whereas the first 300 cm contributed with approximately 76% (2.03 mm/day) (Broedel *et al.*, 2017). However they noticed that during drought events plant water uptake occurred below 480 cm, suggesting these trees might rely on deeper soil water during extreme dry years. A recent study conducted in a seasonal Amazonian forest found a niche segregation of root water uptake in the soil, allowing multi-species coexistence in that forest (Brum *et al.*, 2018). Therefore, we cannot exclude the possibility that the studied trees are using deep water to survive extreme droughts and future studies should investigate the relationship between SWS and SMs along a deeper soil profile. Nonetheless, the studied trees were still operating under negative SMs during the drought (Fig. 4), indicating that the atmospheric water demand was higher than the water supply causing these trees to experience low xylem tensions during the day.

Xylem safety margins can be defined in different ways (Meinzer *et al.*, 2009; Martin-StPaul *et al.*, 2017). Here we used two safety margin metrics: SM_{P50} (Ψ_{min} - Ψ_{50}), which is the most widely used, and SM_{P88} (Ψ_{min} - Ψ_{88}), which is a more conservative safety margin calculation. While negative values of SM_{P50} were recorded during the 2015-2016 drought, SM_{P88} narrowed but were always positive (Fig. 4). In addition, none of the studied trees died during the 2015-2016 El Niño, and were still alive in 2017 (tree mortality of other trees nearby was not evident either), supporting the findings that for angiosperms the lethal level of cavitation is close to 88% of embolized vessels (although this still has not been tested in Amazonian trees; Urli *et al.*, 2013; Delzon & Cochard, 2014; Adams *et al.*, 2017; Choat *et al.*, 2018). Furthermore, during our two-years of Ψ_{leaf} measurements (Fig. 3), we did not register SM_{P50} greater than 1.7 MPa (Fig. 4). These results support the conclusion that most trees operate close to their cavitation threshold

(Choat *et al.*, 2012), probably because narrow SMs maximize gas exchange while avoiding hydraulic failure (Sperry, 2004).

The extreme climatic conditions imposed by the El Niño, caused some trees to cross leaf π_{tlp}, suggesting leaf tissues were also under water stress. The loss of leaf turgor pressure causes leaf wilting resulting in complete stomatal closure (Brodribb *et al.*, 2003; Sack *et al.*, 2003; Bartlett *et al.*, 2012). Our results corroborate other findings that plants can sustain low Ψ_{leaf} for a substantial amount of time and still recover after a re-hydration period (Skelton *et al.*, 2017). The high $\Psi_{predawn}$ values (Fig. 3), suggest that even though plants crossed their π_{tlp} during the day, they were able to re-hydrate at least some of their leaf tissues during the night (through stomatal closure) preventing tree death. Furthermore, when leaf temperature reaches 37-50ºC, which was the case during the 2015-2016 drought (Fig. 2), leaf proteins start to denature, and carbon assimilation processes are impaired (Salvucci *et al.*, 2001; Slot & Winter, 2017). High leaf temperatures are well known to stimulate the overproduction of reactive oxidative species (ROS; Hasanuzzaman *et al.*, 2013), triggering programmed cell death under excessive ROS accumulation (Suzuki *et al.*, 2012). These findings help explain the many upper canopy wilted, and heat damaged leaves observed in the field during the drought. About half of them were able to recover, and the other half dried out and could not regain function.

H2: The decline in sap velocity during the drought will be mainly explained by a decrease in whole-tree hydraulic conductance caused by increased xylem resistance due to a spread in xylem embolism.

As canopy temperature and VPD during the El Niño continued to increase, sap velocity and whole-tree hydraulic conductance (K_{wt}) showed a significant decline (Fig. 5). Under a severe drought, plants can (1) close their stomata to reduce water loss through transpiration, at the cost of carbon assimilation and leaf cooling, (2) leave stomata open (or partially open) and allow xylem tension to increase, risking the integrity of their hydraulic system and (3) can drop all or most of their leaves to prevent further water loss (Cochard *et al.*, 2002; Sperry & Love, 2015; Martin-StPaul *et al.*, 2017). All of these three strategies could cause sap velocity (SV) and K_{wt} to decrease, however, during our study period we did not observe significant leaf loss that may explain the drop in SV [*personal communications K. Jardine and B. Gimenez*]. Therefore, we only considered stomatal resistance and xylem resistance (embolism formation) in our analyses.

To investigate the processes behind the reduction in sap velocity and K_{wt} in our studied trees, we calculated the canopy stomatal ($1/G_s$) and xylem resistances ($1/K_s$) during and after the El Niño. We found that species that crossed their P_{50} (*E. cyathiformis* and *P. anomala*) had high values of $1/K_s$. Canopy stomatal resistance was also high during the El Niño and decreased after the drought. These results suggest that as xylem tension increased and vessels experienced cavitation, plants down-regulated stomatal conductance but were unable to completely prevent xylem embolism. Also, for most of the studied trees, a decline in sap velocity was also observed after individuals reached their P_{50}, and did not go up again to pre-drought values, even when a recovery in precipitation occurred (Fig 5). If only a small portion of the xylem embolizes, the upward movement of water in the tree may continue with minor impact on plant performance (Tyree & Sperry, 1989). However, widespread embolism in the xylem, like we report in

this study, forces trees to operate with less functional xylem, reducing trees' capacity to transport water from the soil to leaves (Sperry & Love, 2015; Cosme *et al.*, 2017), and as a consequence, a decrease in sap velocity and K_{wt} is observed. These findings indicate that daily cavitation and embolism refilling under tension is not routine for these Amazonian trees. Drought-induced xylem cavitation is thus a symptom of distress, and plants would have to rely on the growth of new vessels to continue to transport water (Sperry, 2013; Delzon & Cochard, 2014; Klein *et al.*, 2014).

However, if some of the studied trees were experiencing a dangerous increase in xylem tension, why were they not able to completely close their stomata to prevent further increase in xylem cavitation? A reasonable explanation is that the studied trees may lack the ability to respond rapidly to conserve water under severe droughts. Plants growing in environments where drought events are recurring, usually exhibit rapid stomatal responses to water deficit (Brodribb & Holbrook, 2004; Sperry, 2004). However, wet tropical forests are thermally stable, and large fluctuations in water supply and demand do not frequently occur. Most Amazonian plants may not need to rely on drought-resistance hydraulic strategies to survive drier conditions because of water generally does not represent a limiting resource in rain-forest ecosystems (Janzen, 1967; Doughty & Goulden, 2008). Therefore, the ability of Amazonian trees to survive future climatic events may depend on how well they will be able to acclimate to hotter and drier conditions (Doughty & Goulden, 2008). Another explanation may be the maintenance of transpiration as a leaf thermoregulatory mechanism (Lin *et al.*, 2017). These trees may be favoring to assume hydraulic risks instead of damaging their photosynthetic apparatus. These would be particularly beneficial if trees were able to recover from xylem cavitation, however the ability of plants to refill embolized vessel is still questionable (Cochard & Delzon, 2013).

Although our sample size was limited due to logistical constraints, we report the longest record of diurnal leaf water potential measurements for Amazonian trees to date. We assessed stem and leaf hydraulic response to an extreme climate-change type of drought and demonstrated that five focal Amazonian species are susceptible to climate warming. We would like to point out that our results hold true for the five-individual tree species sampled in this study and more research on the impact of natural droughts on Amazonian trees are needed before any extrapolation is made. Furthermore, linking drought stress vulnerability, with vapor pressure deficit and leaf temperature can strengthen the current understanding of plant function, and facilitate the identification of relationships indicative of ecosystem sensitivity or tolerance to drought. Therefore, studies like ours that measure *in situ* trees' response to a severe drought event are vital if we are to predict what will happen to plant communities under a warmer and drier climate.

References

Adams HD, Zeppel MJ, Anderegg WR, Hartmann H, Landhäusser SM, Tissue DT, Huxman TE, Hudson PJ, Franz TE, Allen CD. 2017. A multi-species synthesis of physiological mechanisms in drought-induced tree mortality. *Nature ecology & evolution* 1(9): 1285.

Allen CD, Breshears DD, McDowell NG. 2015. On underestimation of global vulnerability to tree mortality and forest die-off from hotter drought in the Anthropocene. *Ecosphere* 6(8): 1-55.

Anderegg LD, Anderegg WR, Abatzoglou J, Hausladen AM, Berry JA. 2013. Drought characteristics' role in widespread aspen forest mortality across Colorado, USA. *Global Change Biology* 19(5): 1526-1537.

Anderegg WR, Anderegg LD, Berry JA, Field CB. 2014. Loss of whole-tree hydraulic conductance during severe drought and multi-year forest die-off. *Oecologia* 175(1): 11-23.

Araújo A, Nobre A, Kruijt B, Elbers J, Dallarosa R, Stefani P, Von Randow C, Manzi A, Culf A, Gash J. 2002. Comparative measurements of carbon dioxide fluxes from two nearby towers in a central Amazonian rainforest: The Manaus LBA site. *Journal of Geophysical Research: Atmospheres* 107(D20).

Bartlett MK, Scoffoni C, Sack L. 2012. The determinants of leaf turgor loss point and prediction of drought tolerance of species and biomes: a global meta-analysis. *Ecology Letters* 15(5): 393-405.

Binks O, Meir P, Rowland L, Costa ACL, Vasconcelos SS, Oliveira AAR, Ferreira L, Christoffersen B, Nardini A, Mencuccini M. 2016. Plasticity in leaf-level water relations of tropical rainforest trees in response to experimental drought. *New Phytologist* 211(2): 477-488.

Brodribb T, Holbrook N, Edwards E, Gutierrez M. 2003. Relations between stomatal closure, leaf turgor and xylem vulnerability in eight tropical dry forest trees. *Plant, Cell & Environment* 26(3): 443-450.

Brodribb T, Holbrook NM. 2004. Diurnal depression of leaf hydraulic conductance in a tropical tree species. *Plant, Cell & Environment* 27(7): 820-827.

Broedel E, Tomasella J, Cândido LA, Randow C. 2017. Deep soil water dynamics in an undisturbed primary forest in central Amazonia: Differences between normal years and the 2005 drought. *Hydrological Processes* 31(9): 1749-1759.

Brum M, Vadeboncoeur MA, Ivanov V, Asbjornsen H, Saleska S, Alves LF, Penha D, Dias JD, Aragão LE, Barros F. 2018. Hydrological niche segregation defines forest structure and drought tolerance strategies in a seasonal Amazon forest. *Journal of Ecology*.

Choat B, Brodribb TJ, Brodersen CR, Duursma RA, López R, Medlyn BE. 2018. Triggers of tree mortality under drought. *Nature* 558(7711): 531.

Choat B, Jansen S, Brodribb TJ, Cochard H, Delzon S, Bhaskar R, Bucci SJ, Feild TS, Gleason SM, Hacke UG, et al. 2012. Global convergence in the vulnerability of forests to drought. *Nature* 491(7426): 752-755.

Cochard H, Coll L, Le Roux X, Ameglio T. 2002. Unraveling the Effects of Plant Hydraulics on Stomatal Closure during Water Stress in Walnut. *Plant Physiology* 128(1): 282-290.

Cochard H, Delzon S. 2013. Hydraulic failure and repair are not routine in trees. *Annals of Forest Science* 70(7): 659-661.

Cosme LH, Schietti J, Costa FR, Oliveira RS. 2017. The importance of hydraulic architecture to the distribution patterns of trees in a central Amazonian forest. *New Phytologist*.

Delzon S, Cochard H. 2014. Recent advances in tree hydraulics highlight the ecological significance of the hydraulic safety margin. *New Phytologist* 203(2): 355-358.

Doughty CE, Goulden ML. 2008. Are tropical forests near a high temperature threshold? *Journal of Geophysical Research: Biogeosciences* 113(G1).

Doughty CE, Metcalfe DB, Girardin CA, Amezquita FF, Cabrera DG, Huasco WH, Silva-Espejo JE, Araujo-Murakami A, da Costa MC, Rocha W, et al. 2015. Drought impact on forest carbon dynamics and fluxes in Amazonia. *Nature* 519(7541): 78-82.

Eamus D, Boulain N, Cleverly J, Breshears DD. 2013. Global change-type drought-induced tree mortality: vapor pressure deficit is more important than temperature per se in causing decline in tree health. *Ecology and evolution* 3(8): 2711-2729.

Ewers BE, Oren R. 2000. Analyses of assumptions and errors in the calculation of stomatal conductance from sap flux measurements. *Tree Physiology* 20(9): 579-589.

Gleason SM, Westoby M, Jansen S, Choat B, Hacke UG, Pratt RB, Bhaskar R, Brodribb TJ, Bucci SJ, Cao KF. 2016. Weak tradeoff between xylem safety and xylem-specific hydraulic efficiency across the world's woody plant species. *New Phytologist* 209(1): 123-136.

Gorla L, Signarbieux C, Turberg P, Buttler A, Perona P. 2015. Effects of hydropeaking waves' offsets on growth performances of juvenile Salix species. *Ecological Engineering* 77: 297-306.

Green S, Clothier B, Jardine B. 2003. Theory and practical application of heat pulse to measure sap flow. *Agronomy Journal* 95(6): 1371-1379.

Hacke UG, Stiller V, Sperry JS, Pittermann J, McCulloh KA. 2001. Cavitation fatigue. Embolism and refilling cycles can weaken the cavitation resistance of xylem. *Plant Physiology* 125(2): 779-786.

Hasanuzzaman M, Nahar K, Alam MM, Roychowdhury R, Fujita M. 2013. Physiological, biochemical, and molecular mechanisms of heat stress tolerance in plants. *International Journal of Molecular Sciences* 14(5): 9643-9684.

Higuchi N, Santos J, Lima A, Higuchi F, Chambers JQ. 2011. A floresta Amazônica e a água da chuva. *FLORESTA* 41(3): 417-434.

Hinckley T, Duhme F, Hinckley A, Richter H. 1980. Water relations of drought hardy shrubs: osmotic potential and stomatal reactivity. *Plant, Cell & Environment* 3(2): 131-140.

Irion G, Bush M, De Mello JN, Stüben D, Neumann T, Müller G, Junk J. 2006. A multiproxy palaeoecological record of Holocene lake sediments from the Rio

Tapajós, eastern Amazonia. *Palaeogeography, Palaeoclimatology, Palaeoecology* 240(3): 523-535.

Jacobsen AL, Pratt RB, Davis SD, Ewers FW. 2007a. Cavitation resistance and seasonal hydraulics differ among three arid Californian plant communities. *Plant, Cell & Environment* 30(12): 1599-1609.

Jacobsen AL, Pratt RB, Ewers FW, Davis SD. 2007b. Cavitation Resistance Among 26 Chaparral Species of Southern California. *Ecological monographs* 77(1): 99–115.

Janzen DH. 1967. Why mountain passes are higher in the tropics. *The American Naturalist* 101(919): 233-249.

Jenkins H, Baker P, Guilderson T 2010. Extreme Drought Events Revealed in Amazon Tree Ring Records. *AGU Fall Meeting Abstracts*.

Jiménez-Muñoz JC, Mattar C, Barichivich J, Santamaría-Artigas A, Takahashi K, Malhi Y, Sobrino JA, van der Schrier G. 2016. Record-breaking warming and extreme drought in the Amazon rainforest during the course of El Niño 2015–2016. *Scientific Reports* 6.

Jung M, Reichstein M, Ciais P, Seneviratne SI, Sheffield J, Goulden ML, Bonan G, Cescatti A, Chen J, De Jeu R. 2010. Recent decline in the global land evapotranspiration trend due to limited moisture supply. *Nature* 467(7318): 951-954.

Klein T, Yakir D, Buchmann N, Grünzweig JM. 2014. Towards an advanced assessment of the hydrological vulnerability of forests to climate change-induced drought. *New Phytologist* 201(3): 712-716.

Koide RT, Robichaux RH, Morse SR, Smith CM 1989. Plant water status, hydraulic resistance and capacitance. *Plant physiological ecology*: Springer, 161-183.

Kubiske M, Abrams M. 1991. Rehydration effects on pressure-volume relationships in four temperate woody species: variability with site, time of season and drought conditions. *Oecologia* 85(4): 537-542.

Lewis S, Brando P, M., Phillips O, L., van der Heijden G, M. F. , Nepstad D. 2011. The 2010 Amazon drought. *Science* 331: 554-554.

Lin H, Chen Y, Zhang H, Fu P, Fan Z. 2017. Stronger cooling effects of transpiration and morphology of the plants from a hot dry habitat than from a hot wet habitat. *Functional Ecology*.

Luizão RC, Luizão FJ, Paiva RQ, Monteiro TF, Sousa LS, Kruijt B. 2004. Variation of carbon and nitrogen cycling processes along a topographic gradient in a central Amazonian forest. *Global Change Biology* 10(5): 592-600.

Maréchaux I, Bartlett MK, Sack L, Baraloto C, Engel J, Joetzjer E, Chave J. 2015. Drought tolerance as predicted by leaf water potential at turgor loss point varies strongly across species within an Amazonian forest. *Functional Ecology* 29(10): 1268-1277.

Marengo J, Espinoza J. 2015. Extreme seasonal droughts and floods in Amazonia: causes, trends and impacts. *International Journal of Climatology*.

Marengo JA, Tomasella J, Alves LM, Soares WR, Rodriguez DA. 2011. The drought of 2010 in the context of historical droughts in the Amazon region. *Geophysical Research Letters* 38(12).

Martin-StPaul N, Delzon S, Cochard H. 2017. Plant resistance to drought depends on timely stomatal closure. *Ecology Letters*.

Mayle FE, Power MJ. 2008. Impact of a drier Early-Mid-Holocene climate upon Amazonian forests. *Philos Trans R Soc Lond B Biol Sci* 363(1498): 1829-1838.

McDowell N, Pockman WT, Allen CD, Breshears DD, Cobb N, Kolb T, Plaut J, Sperry J, West A, Williams DG, et al. 2008. Mechanisms of plant survival and mortality during drought: why do some plants survive while others succumb to drought? *New Phytol* 178(4): 719-739.

Meinzer FC, Johnson DM, Lachenbruch B, McCulloh KA, Woodruff DR. 2009. Xylem hydraulic safety margins in woody plants: coordination of stomatal control of xylem tension with hydraulic capacitance. *Functional Ecology* 23(5): 922-930.

Murray FW. 1966. On the computation of saturation vapor pressure: RAND CORP SANTA MONICA CALIF.

Oliveira RS. 2013. Can hydraulic traits be used to predict sensitivity of drought-prone forests to crown decline and tree mortality? *Plant and soil*: 1-3.

Paddock III WA, Davis SD, Pratt RB, Jacobsen AL, Tobin MF, López-Portillo J, Ewers FW. 2013. Factors determining mortality of adult chaparral shrubs in an extreme drought year in California. *Aliso: A Journal of Systematic and Evolutionary Botany* 31(1): 49-57.

Pereira L, Bittencourt PR, Oliveira RS, Junior M, Barros FV, Ribeiro RV, Mazzafera P. 2016. Plant pneumatics: stem air flow is related to embolism–new perspectives on methods in plant hydraulics. *New Phytologist* 211(1): 357-370.

Pereira L, Mazzafera P. 2012. A low cost apparatus for measuring the xylem hydraulic conductance in plants. *Bragantia* 71(4): 583-587.

Powell TL, Wheeler JK, de Oliveira AA, da Costa L, Carlos A, Saleska SR, Meir P, Moorcroft PR. 2017. Differences in xylem and leaf hydraulic traits explain differences in drought tolerance among mature Amazon rainforest trees. *Global Change Biology*.

Sack L, Cowan P, Jaikumar N, Holbrook N. 2003. The 'hydrology'of leaves: co-ordination of structure and function in temperate woody species. *Plant, Cell & Environment* 26(8): 1343-1356.

Salvucci ME, Osteryoung KW, Crafts-Brandner SJ, Vierling E. 2001. Exceptional sensitivity of Rubisco activase to thermal denaturation in vitro and in vivo. *Plant Physiology* 127(3): 1053-1064.

Scholander PF, Hammel H, Bradstreet ED, Hemmingsen E. 1965. Sap pressure in vascular plants. *Science* 148(3668): 339-346.

Skelton RP, Brodribb TJ, McAdam SA, Mitchell PJ. 2017. Gas exchange recovery following natural drought is rapid unless limited by loss of leaf hydraulic conductance: evidence from an evergreen woodland. *New Phytologist* 215(4): 1399-1412.

Slot M, Winter K. 2017. In situ temperature response of photosynthesis of 42 tree and liana species in the canopy of two Panamanian lowland tropical forests with contrasting rainfall regimes. *New Phytologist* 214(3): 1103-1117.

Sombroek W. 2001. Spatial and temporal patterns of Amazon rainfall. Consequences for the planning of agricultural occupation and the protection of primary forests. *Ambio* 30(7): 388-396.

Sperry J. 2013. Cutting-edge research or cutting-edge artefact? An overdue control experiment complicates the xylem refilling story. *Plant, Cell & Environment* 36(11): 1916-1918.

Sperry J, Donnelly J, Tyree M. 1988. A method for measuring hydraulic conductivity and embolism in xylem. *Plant, Cell & Environment* 11(1): 35-40.

Sperry JS. 2004. Coordinating stomatal and xylem functioning–an evolutionary perspective. *New Phytologist* 162(3): 568-570.

Sperry JS, Love DM. 2015. What plant hydraulics can tell us about responses to climate-change droughts. *New Phytologist*.

Stocker TF, Qin D, Plattner G-K, Tignor M, Allen SK, Boschung J, Nauels A, Xia Y, Bex B, Midgley B 2013. IPCC, 2013: climate change 2013: the physical science basis. Contribution of working group I to the fifth assessment report of the intergovernmental panel on climate change: Cambridge University Press.

Suzuki N, Koussevitzky S, Mittler R, Miller G. 2012. ROS and redox signalling in the response of plants to abiotic stress. *Plant, Cell & Environment* 35(2): 259-270.

Trenberth KE, Dai A, Van Der Schrier G, Jones PD, Barichivich J, Briffa KR, Sheffield J. 2014. Global warming and changes in drought. *Nature climate change* 4(1): 17-22.

Trifilò P, Nardini A, Gullo MAL, Barbera PM, Savi T, Raimondo F. 2015. Diurnal changes in embolism rate in nine dry forest trees: relationships with species-specific xylem vulnerability, hydraulic strategy and wood traits. *Tree Physiology* 35(7): 694-705.

Tyree M, Hammel H. 1972. The measurement of the turgor pressure and the water relations of plants by the pressure-bomb technique. *Journal of Experimental Botany* 23(1): 267-282.

Tyree MT, Sperry JS. 1989. Vulnerability of xylem to cavitation and embolism. *Annual review of plant biology* 40(1): 19-36.

Urli M, Porté AJ, Cochard H, Guengant Y, Burlett R, Delzon S. 2013. Xylem embolism threshold for catastrophic hydraulic failure in angiosperm trees. *Tree Physiology* 33(7): 672-683.

Will RE, Wilson SM, Zou CB, Hennessey TC. 2013. Increased vapor pressure deficit due to higher temperature leads to greater transpiration and faster mortality during drought for tree seedlings common to the forest–grassland ecotone. *New Phytologist* 200(2): 366-374.

Williams CB, Reese Næsborg R, Dawson TE. 2017. Coping with gravity: the foliar water relations of giant sequoia. *Tree Physiology* 37(10): 1312-1326.

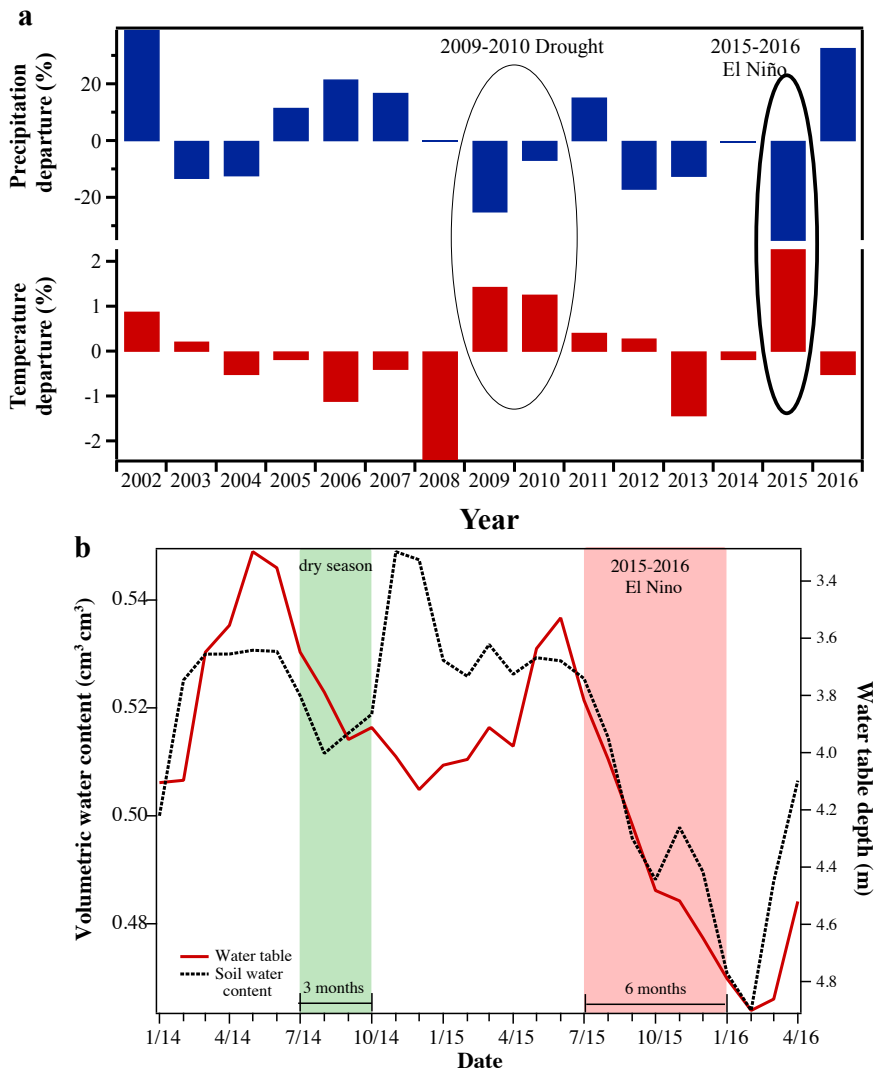

Figure 1. (a) Precipitation and surface air temperature departure from the long-term monthly mean (2002 – 2016) for the period of August-December at the K34 tower. **(b)** Volumetric water content (cm^3 cm^3; VWC) in the first 3m of the soil (black dotted lines), and water table depth (m; WTD; red solid lines) during January 2014 to April 2016. VWC and WTD were measured, respectively, ~150 m and ~500 m from the K34 tower. VWC and WTD have a sharp decrease during the El Niño (red box) compared with the previous dry season of 2014 (green box).

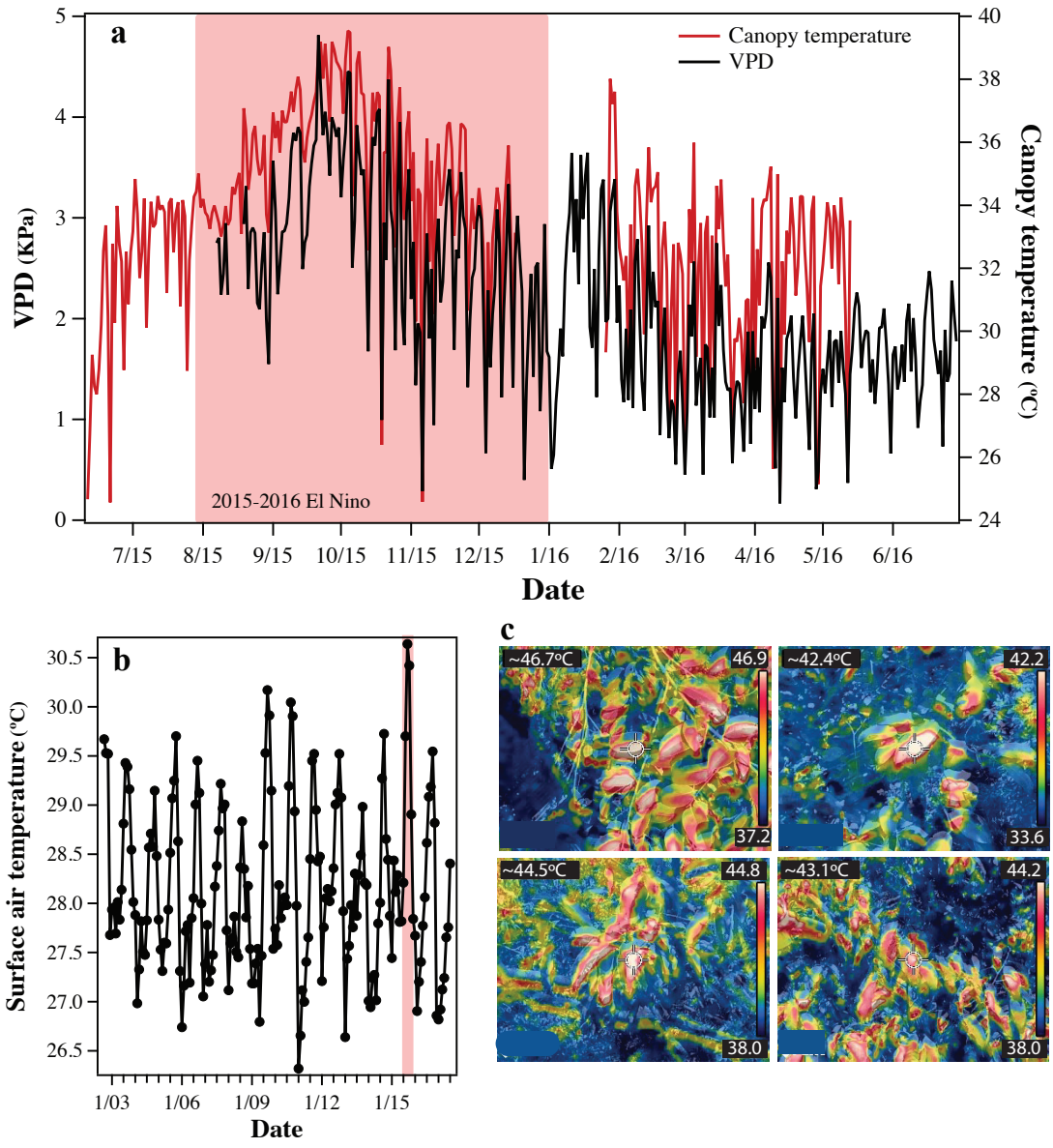

Figure 2. (a) Daily maximum vapor pressure deficit (VPD; black line) and canopy temperature (T_{Canopy}; red line) at the K34 tower from July 2015 to June 2016. **(b)** Landscape scale monthly averaged air surface temperatures at the study site for the period of September 2002 – August 2017. **(c)** Diurnal thermal leaf surface temperature photos taken for each studied species during the peak of the El Niño (September 2015).

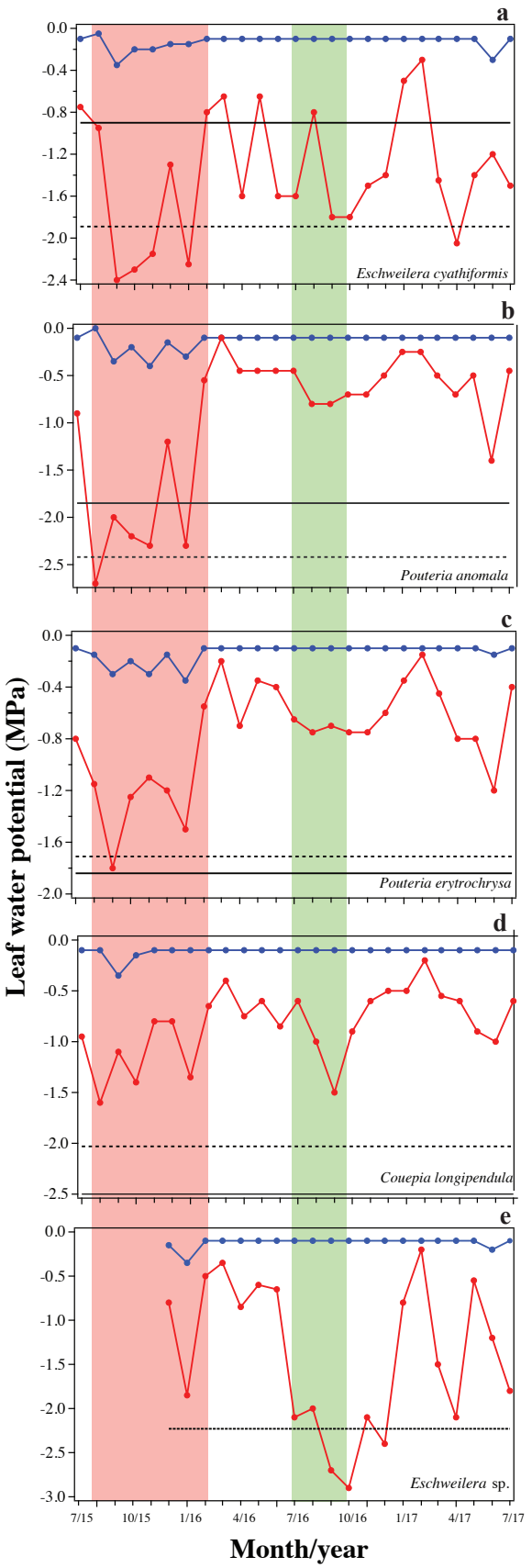

Figure 3. Two years of monthly predawn (blue line) and daily minimum (red line) leaf water potential (July 2015 to July 2017), leaf turgor loss point (dashed black line), 50% loss of hydraulic conductivity (P_{50}; solid black line) for five Amazonian tree species at the K34 tower. The red and green boxes represent the 2015-2016 El Niño and the regular 2016 dry season respectively.

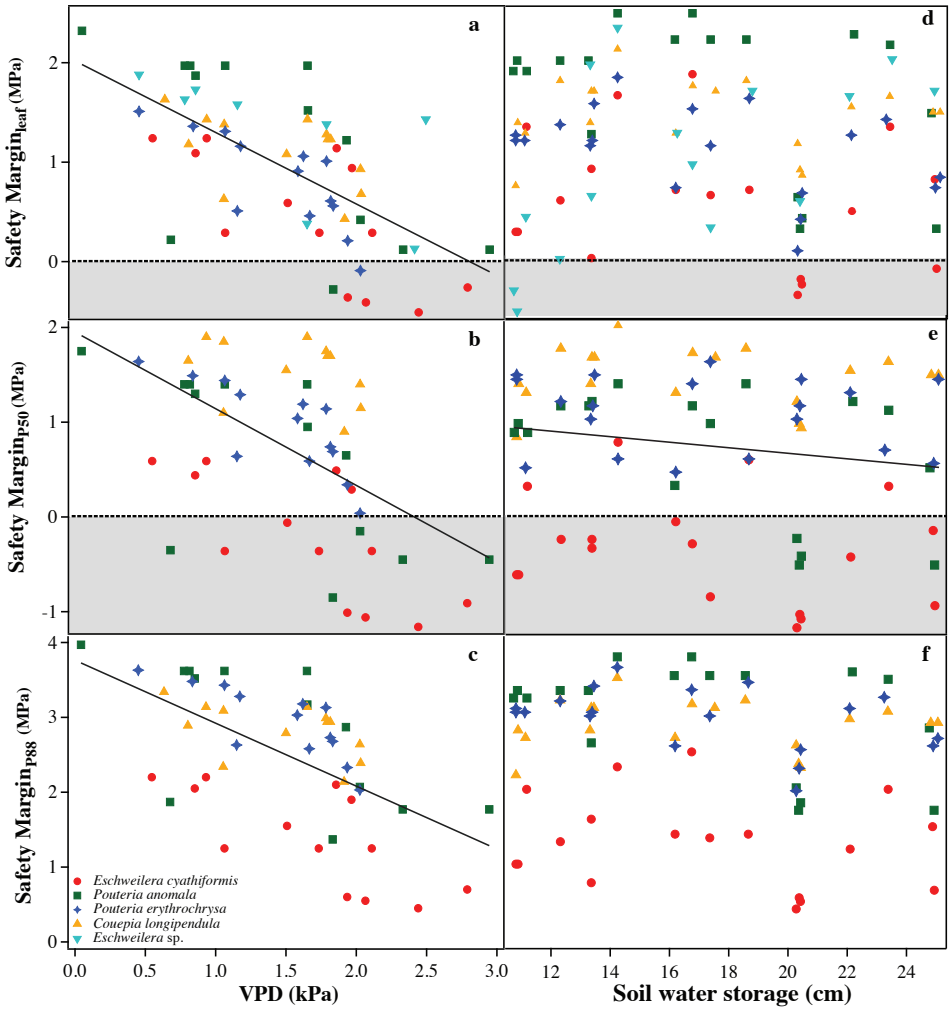

Figure 4. The relationship between **(a-c)** leaf and xylem safety margins and vapor pressure deficit (VPD; n= 52-60) in kPa – species had statistically different intercepts but similar slope, p-value ranged from 1.17 e^{-08} to 6.24 e^{-05}; and **(e-f)** leaf and xylem safety margins and soil water storage (SWS; n=74-89) in cm - The only statistically significant relationship (p-value = 0.0378) was SM_{P50} vs. SWS, where species had random intercepts but the same slope; for five Amazonian tree species at K34 tower. Where leaf safety margin (SM_{leaf}) = Ψ_{TLP} - Ψ_{min}; TLP = leaf turgor loss point; xylem safety margin P_{50} (SM_{P50}) = Ψ_{50} – Ψ_{min}; xylem safety margin P_{88} (SM_{P88}) = Ψ_{80} – Ψ_{min}. The black lines indicate the relationship between SM and canopy temperature without considering species identity. A summary of the statistical results from the best models (lowest AIC values) can be found on the Supplemental information Table S3 and S4.

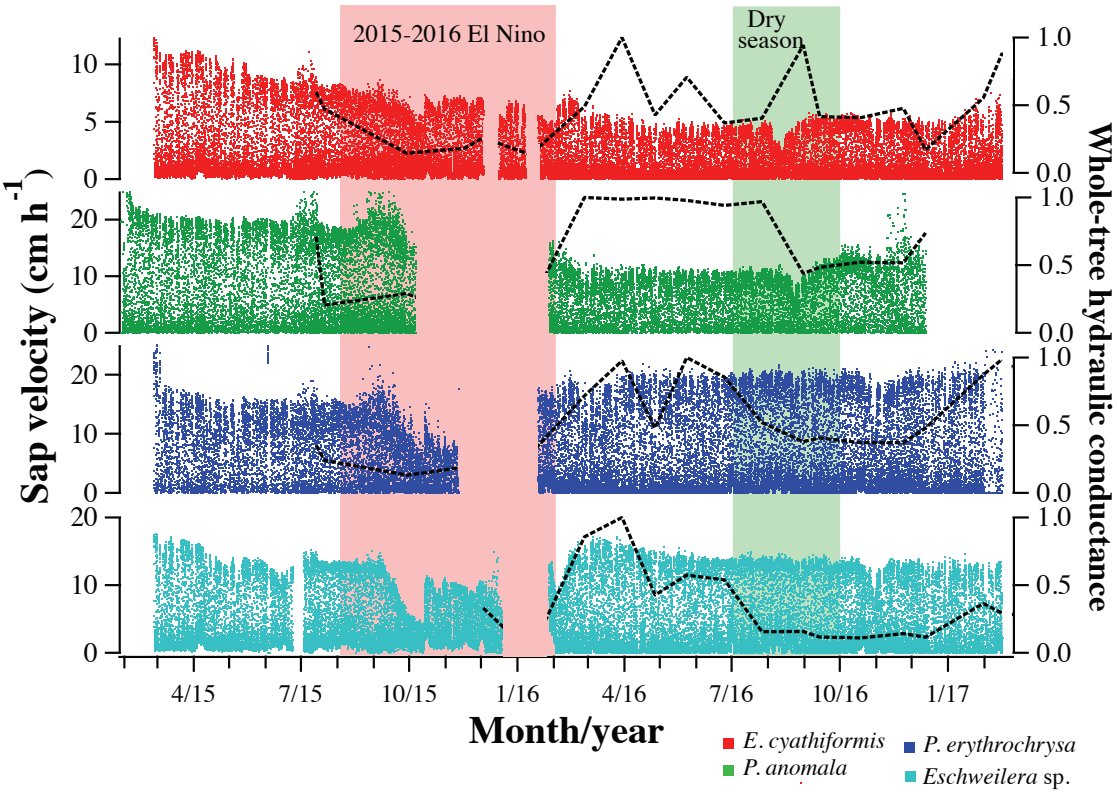

Figure 5. Response and recovery of four Amazonian tree species to the 2015-2016 El Niño in terms of sap velocity (measurements recorded every 5 minutes) and normalized whole-tree hydraulic conductance ($K_{wt}/K_{wt[max]}$; black dashed line). The red and green boxes represent the duration of the 2015-2016 El Niño and the 2016 dry season, respectively. Data gaps represent periods where continuous power was not available and sap velocity could not be measured.

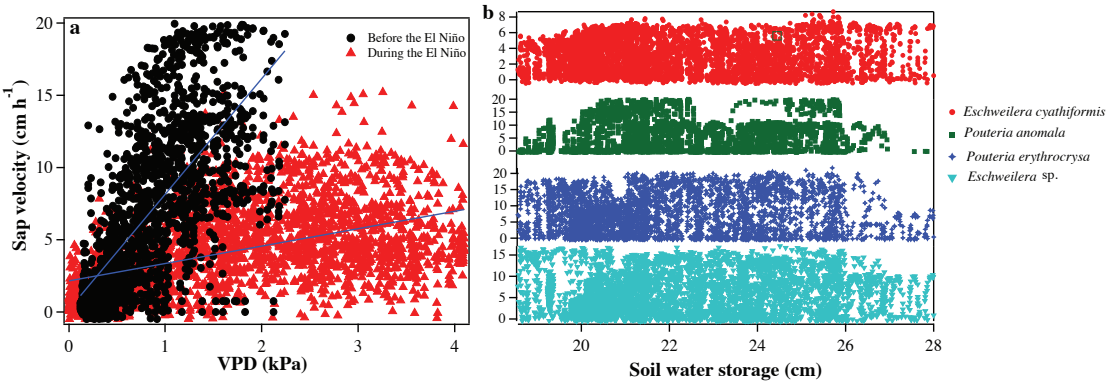

Figure 6. The relationship between (a) sap velocity and vapor pressure deficit (VPD) – a significantly different slope and intercept are observed before (black circles; May and June 2015) and during the peak of the El Niño (red triangles; October 2015); and (b) sap velocity and soil water storage (SWS) in the first 1m, during and before the El Niño (September 2015 – May 2016), for four Amazonian tree specie. The relationship between sap velocity and SWS was not significantly different and species had different intercepts and slopes from each other. Summary of the statistical results can be found in the Supplemental Information Table S6.

CHAPTER 3 A recovery in leaf water potential during midday in Amazonian trees is driven by an imbalance between water demand and supply

Abstract

Water availability is the primary factor limiting terrestrial plant productivity on a global scale. One metric for evaluating how plant-water status may limit plant performance (PP) under water limitation is through fine-scale measurements of leaf water potential (Ψ_L), which reflects the balance between water uptake and water loss. In tropical ecosystems, Ψ_L is assumed to reach its minimum during midday and it is presumed to rarely limit PP. Here, we present *in situ* observations of the diurnal patterns of Ψ_L in conjunction with canopy temperature, vapor pressure deficit (VPD), sap velocity, and leaf-level gas exchange of four central Amazonian species during the dry season. We show a repeatable and dramatic recovery (20-70%) in Ψ_L during midday (11:00-13:00), when Ψ_L is expected to be at its minimum. This recovery pattern was accompanied by an imbalance between stem sap velocity and leaf-level transpiration rates, as evidenced by an increase in the sap velocity/transpiration ratio. Measurements of net photosynthesis peaked in the early morning and were decoupled to transpiration (E) and stomatal conductance (g_s). Photosynthesis showed a clear midday/post-midday depression associated with canopy temperatures exceeding the optimal value for net photosynthesis (~32 °C). Leaf temperature and VPD were higher between 12:00-15:00 when the second decline in Ψ_L was usually observed. This study helps to elucidate the array of processes influencing diurnal patterns of plant-water balance in tropical trees and suggests that one should not assume that Ψ_L in tropical trees reaches its minimum around noon.

Introduction

The fundamental processes that impact the water balance of plants are water uptake, water transport and water loss (Larcher, 2003). The balance becomes negative if water uptake by the roots (e.g. as measured by sap flow) is insufficient to meet the requirements of water loss by transpiration (Tyree, 1997). Transpiration is an inevitable consequence of photosynthesis, but it also has a significant cooling effect (Lambers *et al.*, 2008). In the absence of transpiration, leaf temperature can rapidly rise to potentially lethal levels. Water loss through transpiration commonly shows a high correlation with both leaf temperature and vapor pressure deficit (VPD; Asbjornsen *et al.*, 2011), and leaf stomatal conductance (g_s) can serve as a controlling mechanism which prevents plants from losing too much water (Lange *et al.*, 1971; Jarvis & McNaughton, 1986). As a consequence, the imbalance between water loss and uptake creates a pressure gradient from roots to leaves, which is the driving force of water movement in plants (Wheeler & Stroock, 2008). This pressure gradient is measured through leaf water potential (Ψ_L). A Ψ_L close to zero means little water loss (small potential gradient between soil and leaf) and the more negative Ψ_L is, the lower the sap velocity/transpiration ratio is at a given point in time (Jarvis, 1976; Hölttä & Sperry, 2014). Thus, the flux of water through the soil-plant system is mainly controlled by the rate of water loss through stomata, and leaf

water potential is one of the most useful metrics for evaluating the balance between sap flow (water coming in) and transpiration (water going out of the plant).

The creation of the pressure chamber (Scholander *et al.*, 1965) enabled routine measurements of negative xylem pressures. Since then, leaf and/or xylem water potential has been widely used to estimate plant or soil water status and plant vulnerability to water deficit (Klepper, 1968; Koch *et al.*, 1994; Andrade *et al.*, 1998; Klein, 2014). Studies of diurnal patterns of Ψ_L often show an early morning decline, with a minimum reached during midday in the tropics, and a recovery occurring in the late afternoon as solar radiation decreases (Koch *et al.*, 1994; Hiromi *et al.*, 2012; Barigah *et al.*, 2014). Based on these findings, subsequent studies often measured only predawn (a proxy for soil water potential, Ψ_{soil}) and midday Ψ_L(e.g. Huc *et al.*, 1994; Zhang *et al.*, 2013; Nandanwar *et al.*, 2015). However, Ψ_L can be influenced by many factors (e.g. stomatal conductance, VPD, leaf temperature, soil water availability, rates of nightime sap flow; Dawson *et al.*, 2007) and more detailed diurnal plant-water studies are needed, especially in diverse systems like the Amazonian forest, if species and environmental variability are to be fully understood.

Here we investigate fine-scale (hourly) diurnal patterns of plant water balance of four Amazonian tree species. Our first goal was to characterize the temporal dynamics of water uptake (via sap velocity), water loss (via leaf transpiration), and the consequences of an imbalance between the two on Ψ_L. Second, we wanted to identify the degree to which stomatal behavior and atmospheric water demand regulated water loss in the presence of water deficits and high canopy temperatures.

Because water availability has been shown as a key factor most strongly restricting terrestrial plant production on a global scale (Lambers *et al.*, 2008), studies of plant-water balance will not only benefit our understanding of the diversity of plant responses that impact ecosystem net primary productivity but in our case, will also improve predictions of climate change effects on tropical vegetation. Plant-water information is increasingly being used in vegetation models and is essential in developing and evaluating plant hydraulic subroutines and other emergent model projections (McDowell *et al.*, 2013; Anderegg, 2015; Anderegg *et al.*, 2015; Sperry & Love, 2015; Christoffersen *et al.*, 2016). This is an advantage because changes in ecosystems are often driven by physiological processes at the scale of individuals (Moorcroft *et al.*, 2001), and plant-water use is an important driver of multiple processes at the individual level. Therefore, detailed characterization of plant water balance can also serve as an important benchmark for dynamic vegetation models.

Material and Methods

Study site

The measurements were conducted on four individual trees around the K34 tower (2°35.37′S, 60°06.92′W) in the Reserva Biológica do Cueiras (also known as ZF-2), located 90 km NNW of the city of Manaus, Brazil (Araújo *et al.*, 2002). The site is run by INPA (Instituto Nacional de Pesquisas da Amazonia) under the Large-Scale Biosphere–Atmosphere Experiment in Amazonia (LBA) program. The mean monthly temperature at the study site during our research (July, August and September of 2015) was 27°C, and mean monthly rainfall was 87.97 mm. The dry season is usually between July and September when precipitation is around 100 mm/month (Sombroek, 2001; Higuchi *et al.*,

2011). The vegetation in this area is considered to be undisturbed, mature, terra-firme rainforest, with a leaf area index of 5–6 and an average canopy height of 30 m. The soil on this medium-size plateau area is mainly Oxisols with high clay content (Luizão *et al.*, 2004).

Measurements

Leaf water potential, sap velocity, canopy temperature and vapor pressure deficit: measurements of leaf water potential and sap velocity were made for four species (1 individual/species) around a 55m tower (K34) located 3 km from the ZF@ road inside the forest during the dry season. The species sampled were *Pouteria anomala* ((Pires) T.D.Penn.; Sapotaceae) with 35.3 cm of DBH and 31 m in height, *Pouteria erythrochrysa* (T.D.Penn; Sapotaceae) with DBH = 36.5 cm and 29.3 m height, *Eschweilera cyathiformis* (S.A.Mori; Lecythidaceae) with 14.3 cm of DBH and 19.8 m height, and *Couepia longipendula* (Pilg.; Chrysobalanaceae) with 28.1 cm of DBH and 23.9 m in height. All trees are upper canopy with direct sunlight exposure; the only exception is the individual of *E. cyathiformis* which is a canopy-to-under-story tree (receiving mostly indirect sunlight).

Leaf water potential was diurnally measured using a Scholander pressure chamber (PMS, Corvallis, OR, USA) according to the method described by Scholander *et al.* (1965). Three sun leaves per tree was collected hourly from 6:00 to 18:00 and leaf water potential measurements were made as soon as the leaf was cut from the branch. The leaves were always collected from the same height (± 2m). The Ψ_L measurements were carried on July 14 and August 8 of 2015. In addition to the species sampled at K34 tower, an extra hourly (every hour from 6:00 to 18:00) Ψ_L set of measurements were made in another tower (K14) located ~ 15 Km from K34 where the present study took place. This full-day measurement was carried out on July 29 of 2015 and five tree species were sampled (one individual/species), *Brosimum parinarioides* (Ducke; Moraceae), *Guarea* (F.Allam. ex L) sp. (Meliaceae), *Protium hebetatum* (Daly; Burseraceae), *Lacistema aggregatum* ((P.J.Bergius) Rusby; Lacistemaceae), *Tetragastris panamensis* ((Engl.) Kuntze; Burseraceae). All these individuals are upper canopy trees and receive direct sunlight throughout day. We wanted to investigate if the diurnal patterns of Ψ_L recorded for the four species studied at K34 were representative and if similar pattern is found for species located in a different area.

Sap velocity was continuously monitored in the main trunk (~1.3 m above the ground) of each of the four K34 study trees, every 15 min during the dry season (July to August of 2015) using Heat Ratio Method sensors (HRM-sensors; ICT International Ltd, Armidale, NSW, Australia;Burgess *et al.*, 2001). HRM probes measured sap velocity at two radial depths in the xylem: 0.75 (outer sensor) and 2.25 cm (inner sensor). The inner sensor data presented problems due to latex exudation for the species *Pouteria anomala* and *P. erythrochrysa* so in this study only the outer sensor data was used. The sap velocity was calculated using the software Sap Flow Tool version 1.1.4 (ICT International Ltd, Armidale, NSW, Australia).

Canopy surface temperature (T_{Canopy}) was measured continuously from July to August of 2015, every five minutes using five infrared radiometers (IR) sensor (SI-111, Apogee Inc). The sensors were installed on the K34 tower at 21.8, 22.8, 24.0, 25.3, and 28.8 m height, using 2 m aluminum poles that extended into the forest canopy. Each sensor was mounted at the end of the aluminum pole, at a ~45-degree angle, pointed at a target leaf cluster. Each sensor was placed ~20

cm from the target to limit field of view errors. The two lowest sensors (i.e., below 24 m) were characterized as partially sunlit leaves measurements, while the three highest sensors were fully sunlit leaves. A CR-3000 datalogger (Campbell Scientific) was used to store the T_{canopy} data. Except *E. cyathiformis*, the only species that is an understory tree, all of the T_{canopy} measurements corresponded to the same study trees in which Ψ_L and sap velocity were recorded.

Vapor pressure deficit (VPD) data were made available by the LBA program (Instituto Nacional de Pesquisas da Amazônia – INPA) and were obtained from the micrometeorological station located at K34 tower. VPD was calculated using air temperature and relative humidity data collected at 35.3m height, every 30 minutes (average of 30 points gathered during the 30 minute period) and using thermo-hygrometers (HMP45AC, Vaisala Inc., Woburn, MA, USA).

Leaf gas exchange measurements: Diurnal patterns of net leaf photosynthesis (*A*), stomatal conductance (g_s) and transpiration (*E*) were measured continuously (5:00-17:00) from fully-developed leaves of *Pouteria anomala* at ~ 25m height. A portable photosynthesis system (Licor 6400XT, Licor, Lincoln, NE, USA) was installed on the tower at the appropriate height with the leaf chamber head extended up to 1 meter from the tower using a Magic Arm (Manfroto, Italy). Natural sunlight was used as the light source (clear top chamber), CO_2 in the reference line was held constant at 400 ppm, and the air flow rate entering the chamber was held constant at 400 micromol/min. Leaf temperature was kept constant during each measurement period and set to values that were determined based on readings of the CST system described above. Once the set leaf temperature stabilized, the IRGAs (Infrared gas analyzer) were matched and a leaf was placed in the chamber and data was recorded every 15 seconds for 10 minutes. Following this, the data logging was paused, and the leaf was removed before setting a new leaf temperature and repeating the cycle. Stabilization of the new leaf temperature was rapid in the morning when temperatures were < 30 ^{o}C but required up to 20-30 minutes to stabilize in the afternoon once leaf temperatures reached values over 35 ^{o}C. For each measurement cycle, a new leaf was chosen from one of the several branches near the tower and repeat measurements on each leaf (15-20 total) were made in the morning and afternoon. Gas-exchange measurements for *P. anomala* leaves were carried out on September 3, of 2015.

Results

Diurnal patterns of leaf water potential, sap velocity, canopy surface temperature and vapor pressure deficit

During July and August of 2015, daily minimum leaf water potential (Ψ_L) varied from -0.6 to -2.4 MPa. The species *Pouteria anomala* had the most negative Ψ_L registered during this period (Figure 1). For all species, Ψ_L showed a rapid decline in early morning followed by dramatic recoveries (20-70% of the minimum early morning value) around mid-day. During the afternoon, a second decline in Ψ_L was usually observed with a full recovery in the evening (Figure 1).

Diurnal measurements of Ψ_L were also made for the same individuals one year later (July and August 2016), and a similar pattern was found (S1 Supplementary Materials). Also, to test if the same trend was observed for other tree species in the area, on July 29, 2015 we measured Ψ_L of an additional five species located around the K14

tower, ~15 km away from the studied trees, and similar results were found (Figure 2), demonstrating a general pattern of Ψ_L recovery around the noon hour.

Maximum sap velocity varied from 8.86 (*E. cyathiformis*) to 19.78 $cm.h^{-1}$ (*Couepia longipendula*) and started to increase as soon as the Ψ_L went down (Figure 1). Even with its tight relationship with Ψ_L (the gradient between Ψ_L and Ψ_{soil} is the driving force for the movement of water), sap velocity did not show large oscillations during the day as observed for Ψ_L and it only decreased at the end of the day (after 16:00) when plants were well hydrated (Figure 1). Also, sap velocities near the ground (~1.5m) had a strong correlation (r = 0.87) with canopy temperature in the upper canopy (~25 m).

Canopy temperature (T_{canopy}) showed a steady increase until 10:00 when it starts to oscillate from 28 to 34 ºC until reaching its daily maximum between 12:00-15:00 (Figure 1), which is when the second decline in Ψ_L was usually observed. Vapor pressure deficit (VPD) also reached its daily maximum between 12:00-15:00 when atmospheric demand for water was highest (Figure 1 and data not shown). VPD showed a strong, positive correlation with sap velocity for all four species (Figure 3 left panels), however, this relationship changes during the day (Figure 3 right panels). From 6:00 to 11:30 there was a positive correlation between VPD and sap velocity, but from 11:00 to noon this relationship started to shift, and this was usually the time when we observed the recovery in Ψ_L. From 12:00 to 15:30 sap velocity did not respond as positively to an increase in VPD, and this was when the second decline in Ψ_L was noticed (Figure 3). After 16:00 as VPD declined, sap velocity also decreased and a recovery in Ψ_L was observed. Even though this pattern was detected for all four species, there was substantial variation in VPD dynamics for the different plants. The species *Couepia longipendula* and *Pouteria anomala* were more responsive to an increase in VPD (sharp increase in sap velocity until it reached a plateau), while *Eschweilera cyathiformis* and *Pouteria erythrochrysa* were slower in responding to changes in VPD and did not reach an apparent plateau like the other two species (Figure 3).

Transpiration, photosynthesis and stomatal conductance

Detailed temporally-resolved diurnal observations of leaf gas exchange in the species *Pouteria anomala* revealed peaks in net photosynthesis (*A*) in the morning (9:00-10:00) followed by a slow decline during the day (Figure 4, Table 1). *A* decreased ~50% from between ~9:30 to ~10:30, the peak of leaf transpiration (*E*) and ~ 30 to 80% during the peak of T_{canopy} and VPD. Thus, a suppression of net photosynthesis was observed from 12:00 to early afternoon during the hottest part of the day, usually after T_{leaf} reached ~ 35ºC (Figure 4). Even though *A* decreased after midday, stomatal conductance (g_s) did not show large oscillations after ~11:00, suggesting that stomata were not completely closing. On the other hand, *E* followed VPD and leveled off after noontime. Therefore, *A* and *E* were decoupled from each other (Figure 4, green and blue boxes). *A* was correlated more with T_{leaf} than by g_s, suggesting a biochemical regulation, whereas *E* was driven mainly by the interaction of conductance and VPD.

Discussion

Because photosynthesis (*A*), stomatal conductance (g_s), transpiration (*E*), canopy temperature (T_{canopy}) and vapor pressure deficit (VPD) increased in the morning, a rapid decline in leaf water potential (Ψ_L) was observed, which has also been reported in other

tropical studies (Koch *et al.*, 1994; Brodribb & Holbrook, 2004; Fisher *et al.*, 2006; Hiromi *et al.*, 2012; Barigah *et al.*, 2014). However, what has not been described in previous studies is a partial recovery (20-70%) in Ψ_L around the solar noon when most plants have hit their peak water deficit (atmospheric water demand is increasing but water supply is not) and would therefore not be expected to have the capacity to recover. Two declines in Ψ_L were detected during the day with a recovery occurring around mid-day (Figure 1). Moreover, this surprising result was not restricted to the trees close to the K34 tower (S1 - supplementary materials). In July, 2015 diurnal Ψ_L measurements of five different trees species around the K14 tower showed similar results (Figure 2). Furthermore, for some of the tropical studies that have been reviewed, hourly values of Ψ_L have been observed to recover around noon. For example, Fisher *et al.* (2006) found that one of their study trees in the east Amazon showed a gradual recovery in Ψ_L throughout the afternoon and a *Dipterocarpus pachyphyllus* tree studied in a Borneo forest also presented a similar pattern in Ψ_L as described here (Hiromi *et al.*, 2012). Therefore, a recovery in Ψ_L around midday may be a general pattern that has not been widely recognized.

The first decrease in Ψ_L occurred just around the time *A,* g_s, and *E* were at their highest values (9:00 – 11:00; Figure 1 and 4). During this period, canopy temperature and VPD increase and even though they had not reached their daily maximum just yet, the water exiting through *E* was enough to increase the gradient between Ψ_L and the soil water potential (Klepper, 1968; Zhang *et al.*, 2013). As a result, sap velocity (and thus water flow) showed a sharp increase, and more water began to flow from the soil to the plants (Figure 1). Therefore, the first decline in Ψ_L typically occurred during the peak of *A* and *E*, but before the maximum daily canopy temperature (~ 35 ºC) and vapor pressure deficit (VPD ~ 3 kPa) was reached, which was around 12:00-15:00 (Figure 1).

After the first early morning decline, Ψ_L was not constant throughout the rest of the day as expected and reported by studies from temperate environments (Klepper, 1968). On the contrary, an increase in Ψ_L ranging from 20-70% was clearly documented. This partial recovery in Ψ_L around noon is probably the result of an imbalance between water coming in through sap velc and water being lost by transpiration. After ~11:00 photosynthesis decreased while *E* and g_s showed a small reduction before stabilizing (*E* increases again around 14:00), however, T_{canopy} and VPD had not yet reached their maximum. During this 'window of time' water was still going in through sap velocity (sap velocity showed little variation during the day) but the amount of water being lost through *E* decreased due to a reduction in conductance (note: $E = \Delta VPD \times g_{total}$). Furthermore, sap velocity and VPD from 6:00 to 11:30 showed a positive relationship (Figure 3 blue dots) suggesting that during this time frame water was not limited. Consequently, we observed a recovery of Ψ_L around noon. It is important to note that the time of the declines and the recovery periods in Ψ_L may vary among species and on different days because environmental conditions do change. However, for all trees during 6:00 – 18:00, we consistently observed the two declines in Ψ_L and a recovery period between them.

A second decline in Ψ_L followed the recovery described above, and it usually occurred during a peak in both T_{canopy} and VPD (Figure 1). This decline was expected because the gradient between leaf and air moisture increased and therefore intensified, and as a result high transpiration rates were observed even though stomata conductance

stayed relatively constant ($E = \Delta VPD \times g_{total}$). Also, the relationship between VPD and sap velocity in the afternoon decreased in a different trajectory than it increased, suggesting that from ~ noon to 18:00 (Figure 2 red dots) less water is available for plants. After the second decline in Ψ_L the xylem tension started to slowly become less negative again, VPD and transpiration decreased and by 18:00 the trees were usually well hydrated. The hysteresis detected between sap velocity, VPD, T_{canopy} and stomatal conductance for the four species, is discussed in detail by Gimenez *et al.* (*in preparation*).

These findings raise the question of why this recovery period in Ψ_L has not been described before. Our data suggest that the observed patterns may result from the plant's inability to maintain a favorable Ψ_L and therefore sufficient leaf turgor to permit leaf stomata to remain open. Alternatively, when demand for canopy water exceeds its supply, appropriate recharge of depleted water stores in the functional xylem could lead to an over all hydraulic limitation and the patterns of sap velocity and water potentials that we observed. Those species with high water transport capacity would be able to replace water that is lost through transpiration more quickly, and therefore, a recovery would be seen just before the maximum transpiration rate is achieved (Brodribb *et al.*, 2007; Campanello *et al.*, 2008). Because our investigation sampled a wide range of phylogenetic groups it seems unlikely that these patterns (e.g. isohydric and anisohydric species or hydraulic strategies) are species specific. It is also important to note that only a small number of tropical studies (e.g. Fisher *et al.*, 2006) have actually measured Ψ_L on an hourly basis, and hardly any studies have done so in Amazonian forests. Most studies collect Ψ_L only during the early morning (pre-dawn), mid-day, and late afternoon (e.g. Huc *et al.*, 1994; Zhang *et al.*, 2013). As a result, previous findings would not have detected the types of patterns we have reported here and therefore could have underestimated the minimum daily Ψ_L, because our study clearly shows that plants do not necessarily reach their minimum around solar noon. Instead, studies that aim to capture the lowest Ψ_L of the day should make multiple measurements between 11:00 – 15:00.

Our findings also suggest that dynamic vegetation models may need to be refined since credible simulations of soil-plant-atmosphere interaction require that diurnal patterns of Ψ_L, g_s, transpiration, photosynthesis and sap velocity be characterized in terms of process parameterization and assumptions to correctly interpret the projections of future vegetation changes (Christoffersen *et al.*, 2016). For example, Anderegg *et al.* (2017) found AIC differences greater than 3 when they considered plant hydraulics (e.g. leaf water potential) into the Ball-Berry-Leuning model. In conclusion, this study sheds new light on how patterns of leaf water potential are driven by the imbalance between leaf transpiration and sap velocity in tropical zones. We suggest that researchers consider including hourly assessment of Ψ_L in their study design and caution that previous approaches that estimate minimum Ψ_L in tropical trees using midday measurements are likely to underestimate minimum water potential.

References

Anderegg WR. 2015. Spatial and temporal variation in plant hydraulic traits and their relevance for climate change impacts on vegetation. *New Phytologist* 205(3): 1008-1014.

Anderegg WR, Flint A, Huang C-y, Flint L, Berry JA, Davis FW, Sperry JS, Field CB. 2015. Tree mortality predicted from drought-induced vascular damage. *Nature Geoscience* 8(5): 367-371.

Anderegg WR, Wolf A, Arango-Velez A, Choat B, Chmura DJ, Jansen S, Kolb T, Li S, Meinzer F, Pita P. 2017. Plant water potential improves prediction of empirical stomatal models. *PloS one* 12(10): e0185481.

Andrade JL, Meinzer FC, Goldstein G, Holbrook NM, Cavelier J, Jackson P, Silvera K. 1998. Regulation of water flux through trunks, branches, and leaves in trees of a lowland tropical forest. *Oecologia* 115(4): 463-471.

Araújo A, Nobre A, Kruijt B, Elbers J, Dallarosa R, Stefani P, Von Randow C, Manzi A, Culf A, Gash J. 2002. Comparative measurements of carbon dioxide fluxes from two nearby towers in a central Amazonian rainforest: The Manaus LBA site. *Journal of Geophysical Research: Atmospheres* 107(D20).

Asbjornsen H, Goldsmith GR, Alvarado-Barrientos MS, Rebel K, Van Osch FP, Rietkerk M, Chen J, Gotsch S, Tobon C, Geissert DR. 2011. Ecohydrological advances and applications in plant–water relations research: a review. *Journal of Plant Ecology* 4(1-2): 3-22.

Barigah TS, Aussenac G, Baraloto C, Bonal D, Cochard H, Granier A, Guehl J-M, Huc R, Sobrado MA, Tyree M. 2014. The water relations of two tropical rainforest species (Virola surinamensis and Eperua falcata): Is Virola unusual as previously reported? *Journal of Plant Hydraulics* 1: e0002.

Brodribb T, Holbrook NM. 2004. Diurnal depression of leaf hydraulic conductance in a tropical tree species. *Plant, Cell & Environment* 27(7): 820-827.

Brodribb TJ, Feild TS, Jordan GJ. 2007. Leaf maximum photosynthetic rate and venation are linked by hydraulics. *Plant Physiology* 144(4): 1890-1898.

Burgess SS, Adams MA, Turner NC, Beverly CR, Ong CK, Khan AA, Bleby TM. 2001. An improved heat pulse method to measure low and reverse rates of sap flow in woody plants. *Tree Physiology* 21(9): 589-598.

Campanello PI, Gatti MG, Goldstein G. 2008. Coordination between water-transport efficiency and photosynthetic capacity in canopy tree species at different growth irradiances. *Tree Physiology* 28(1): 85-94.

Christoffersen BO, Gloor M, Fauset S, Fyllas NM, Galbraith DR, Baker TR, Kruijt B, Rowland L, Fisher RA, Binks OJ. 2016. Linking hydraulic traits to tropical forest function in a size-structured and trait-driven model (TFS v. 1-Hydro). *Geoscientific Model Development* 9(11): 4227.

Dawson TE, Burgess SS, Tu KP, Oliveira RS, Santiago LS, Fisher JB, Simonin KA, Ambrose AR. 2007. Nighttime transpiration in woody plants from contrasting ecosystems. *Tree Physiology* 27(4).

Fisher RA, Williams M, DO V, LOBO R, DA COSTA AL, MEIR P. 2006. Evidence from Amazonian forests is consistent with isohydric control of leaf water potential. *Plant, Cell & Environment* 29(2): 151-165.

Higuchi N, Santos J, Lima A, Higuchi F, Chambers JQ. 2011. A floresta Amazônica e a água da chuva. *FLORESTA* 41(3): 417-434.

Hiromi T, Ichie T, Kenzo T, Ninomiya I. 2012. Interspecific variation in leaf water use associated with drought tolerance in four emergent dipterocarp species of a tropical rain forest in Borneo. *Journal of forest research* 17(4): 369-377.

Hölttä T, Sperry J 2014. Plant water transport and cavitation. *Transport and Reactivity of Solutions in Confined Hydrosystems*: Springer, 173-181.

Huc R, Ferhi A, Guehl J. 1994. Pioneer and late stage tropical rainforest tree species (French Guiana) growing under common conditions differ in leaf gas exchange regulation, carbon isotope discrimination and leaf water potential. *Oecologia* 99(3-4): 297-305.

Jarvis P. 1976. The interpretation of the variations in leaf water potential and stomatal conductance found in canopies in the field. *Philosophical Transactions of the Royal Society of London B: Biological Sciences* 273(927): 593-610.

Jarvis PG, McNaughton K. 1986. Stomatal control of transpiration: scaling up from leaf to region. *Advances in ecological research* 15: 1-49.

Klein T. 2014. The variability of stomatal sensitivity to leaf water potential across tree species indicates a continuum between isohydric and anisohydric behaviours. *Functional Ecology* 28(6): 1313-1320.

Klepper B. 1968. Diurnal pattern of water potential in woody plants. *Plant Physiology* 43(12): 1931-1934.

Koch GW, Amthor JS, Goulden ML. 1994. Diurnal patterns of leaf photosynthesis, conductance and water potential at the top of a lowland rain forest canopy in Cameroon: measurements from the Radeau des Cimes. *Tree Physiology* 14(4): 347-360.

Lambers H, Chapin III FS, Pons TL 2008. Plant water relations. *Plant Physiological Ecology*: Springer, 163-223.

Lange OL, Lösch R, Schulze E-D, Kappen L. 1971. Responses of stomata to changes in humidity. *Planta* 100(1): 76-86.

Larcher W. 2003. *Physiological plant ecology: ecophysiology and stress physiology of functional groups*: Springer Science & Business Media.

Luizão RC, Luizão FJ, Paiva RQ, Monteiro TF, Sousa LS, Kruijt B. 2004. Variation of carbon and nitrogen cycling processes along a topographic gradient in a central Amazonian forest. *Global Change Biology* 10(5): 592-600.

McDowell NG, Fisher RA, Xu C, Domec J-C, Hölttä T, Mackay DS, Sperry JS, Boutz A, Dickman L, Gehres N. 2013. Evaluating theories of drought-induced vegetation mortality using a multimodel–experiment framework. *New Phytologist* 200(2): 304-321.

Moorcroft P, Hurtt G, Pacala SW. 2001. A method for scaling vegetation dynamics: the ecosystem demography model (ED). *Ecological monographs* 71(4): 557-586.

Nandanwar HR, Manivel P, Saravanan R, Shah S, Ravi V. 2015. Photosynthetic Performance and its Relationship with Leaf Water Potential in Desmodium gangeticum L. DC.(Shalaparni) Genotypes under Field Conditions. *Molecular Plant Breeding* 6.

Scholander PF, Hammel H, Bradstreet ED, Hemmingsen E. 1965. Sap pressure in vascular plants. *Science* 148(3668): 339-346.

Sombroek W. 2001. Spatial and temporal patterns of Amazon rainfall. Consequences for the planning of agricultural occupation and the protection of primary forests. *Ambio* 30(7): 388-396.

Sperry JS, Love DM. 2015. What plant hydraulics can tell us about responses to climate-change droughts. *New Phytologist*.

Tyree MT. 1997. The cohesion-tension theory of sap ascent: current controversies. *Journal of Experimental Botany* 48(10): 1753-1765.

Wheeler TD, Stroock AD. 2008. The transpiration of water at negative pressures in a synthetic tree. *Nature* 455(7210): 208-212.

Zhang YJ, Meinzer FC, QI JH, Goldstein G, CAO KF. 2013. Midday stomatal conductance is more related to stem rather than leaf water status in subtropical deciduous and evergreen broadleaf trees. *Plant, Cell & Environment* 36(1): 149-158.

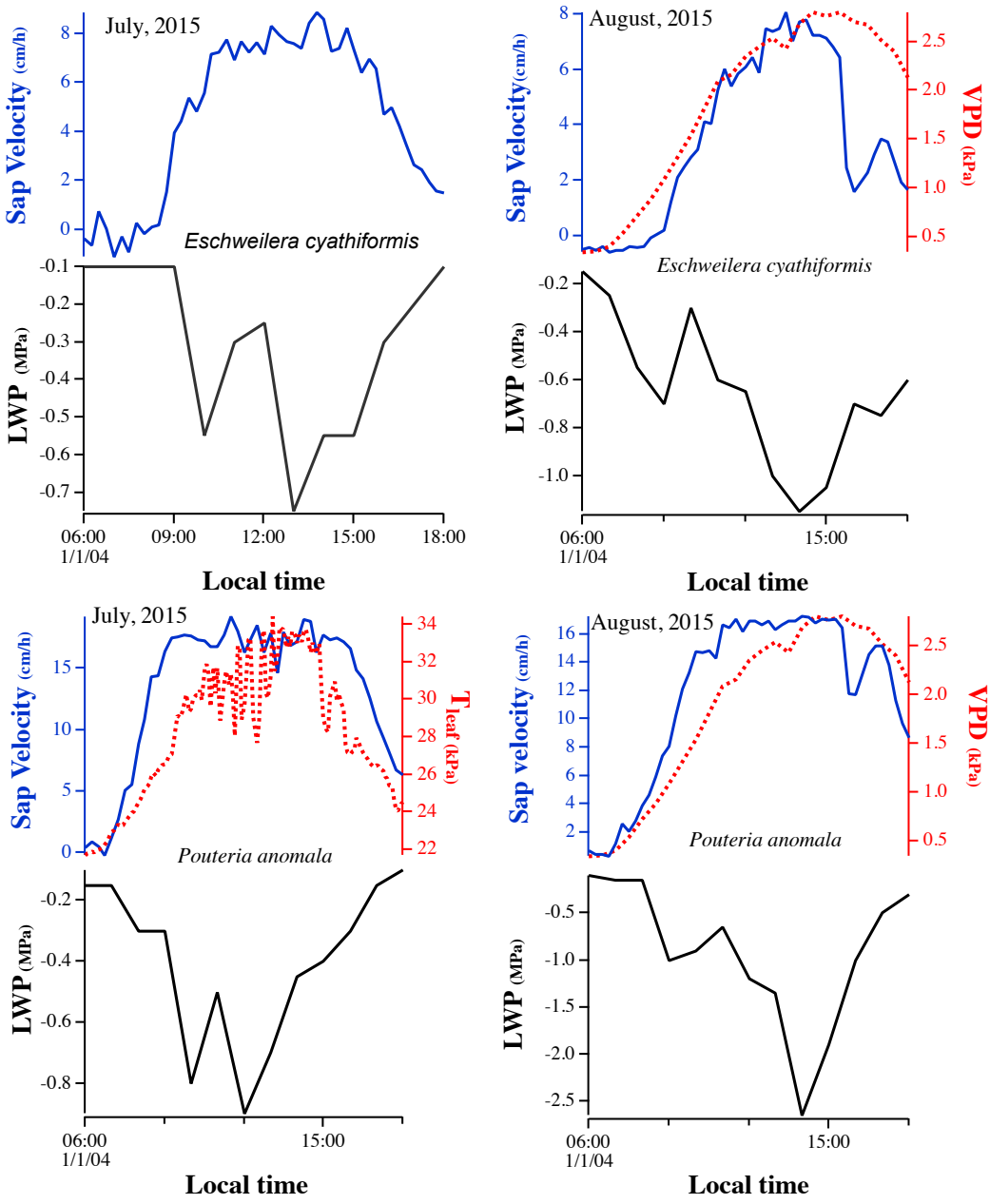
July, 2015
Sap Velocity (cm/h)
Eschweilera cyathiformis
LWP (MPa)
06:00
1/1/04
09:00
12:00
15:00
18:00
Local time
August, 2015
Sap Velocity(cm/h)
VPD (kPa)
Eschweilera cyathiformis
LWP (MPa)
06:00
1/1/04
15:00
Local time
July, 2015
Sap Velocity (cm/h)
T leaf (kPa)
Pouteria anomala
LWP (MPa)
06:00
1/1/04
15:00
Local time
August, 2015
Sap velocity (cm/h)
VPD (kPa)
Pouteria anomala
LWP (MPa)
06:00
1/1/04
15:00
Local time

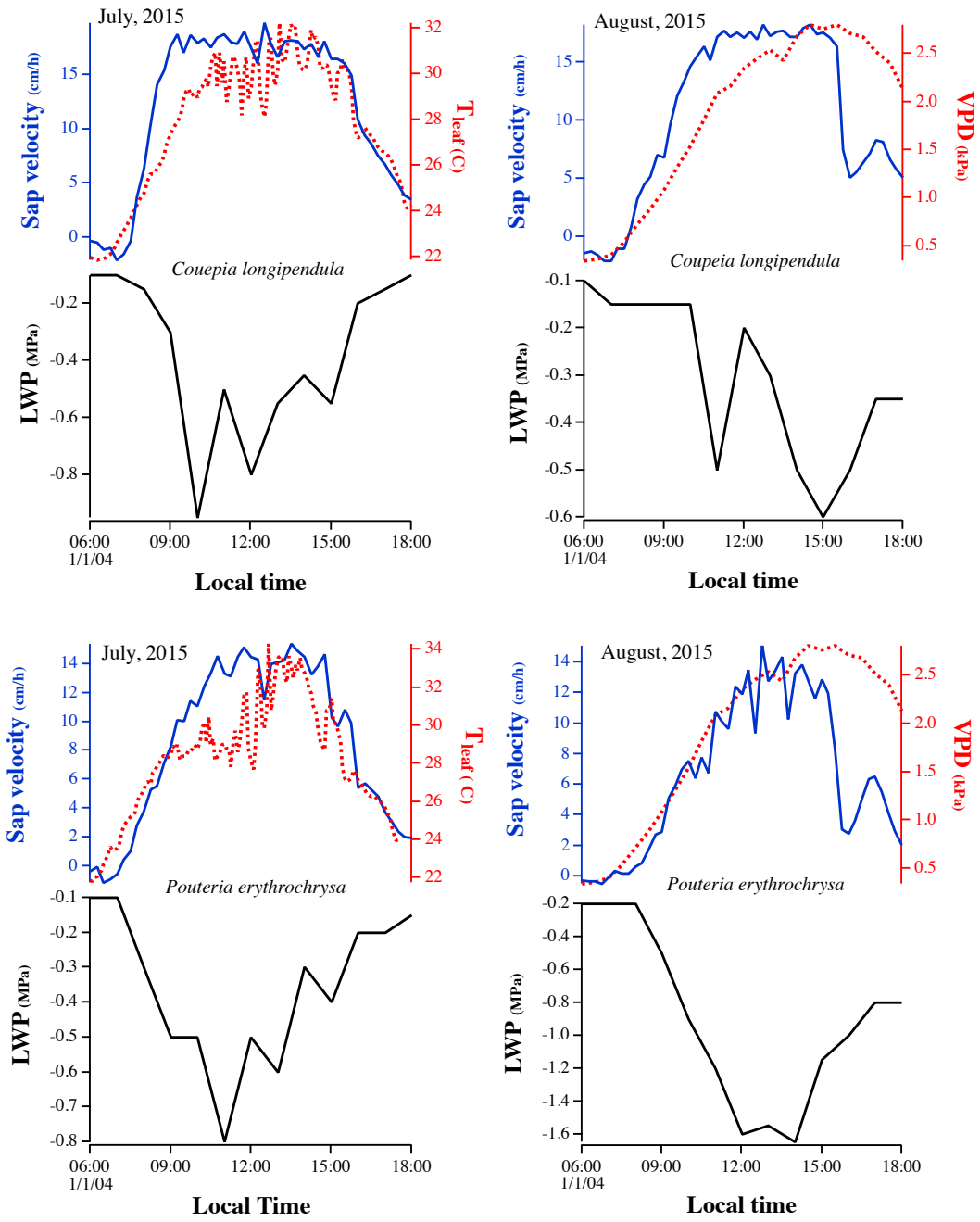

Figure 1. Diurnal patterns of canopy temperature (T_{leaf}), sap velocity, vapor pressure deficit (VPD) and leaf water potential of four tree species (*Eschweilera cyathiformis*, *Pouteria anomala*, *Couepia longipendula* and *Pouteria erythrochrysa*) in a Central Amazonian forest during July (left panels) and August (right panels) of 2018.

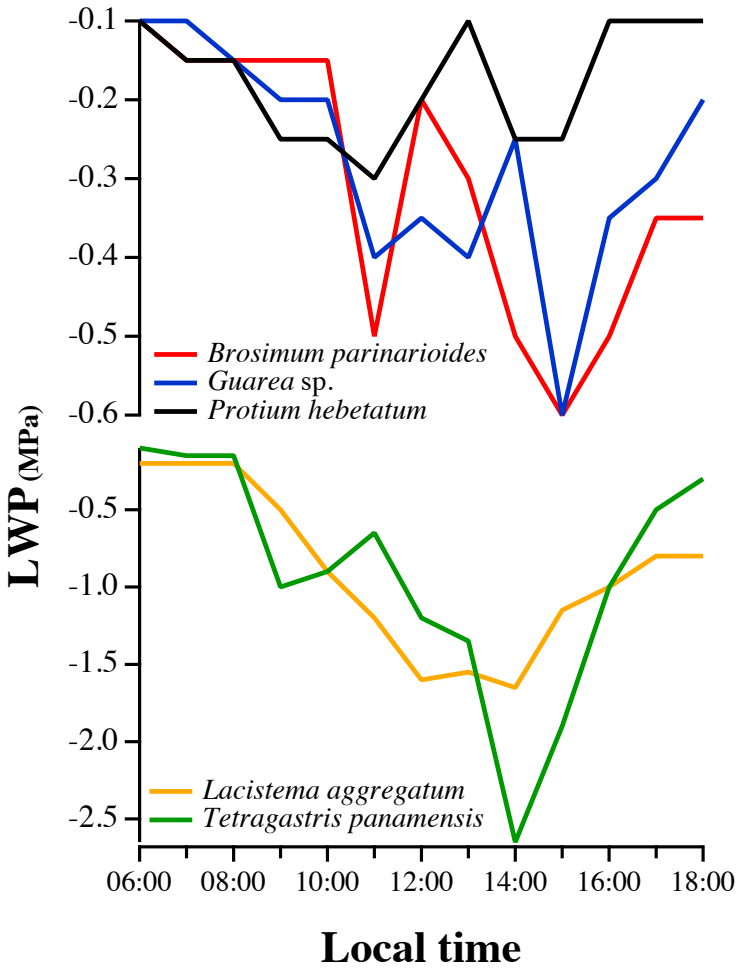

Figure 2. Diurnal patterns of leaf water potential of an additional five tree species around the K14 tower, located 15 Km apart from the K34 tower where the study was conducted. The measurements were carried on in July 29 of 2015.

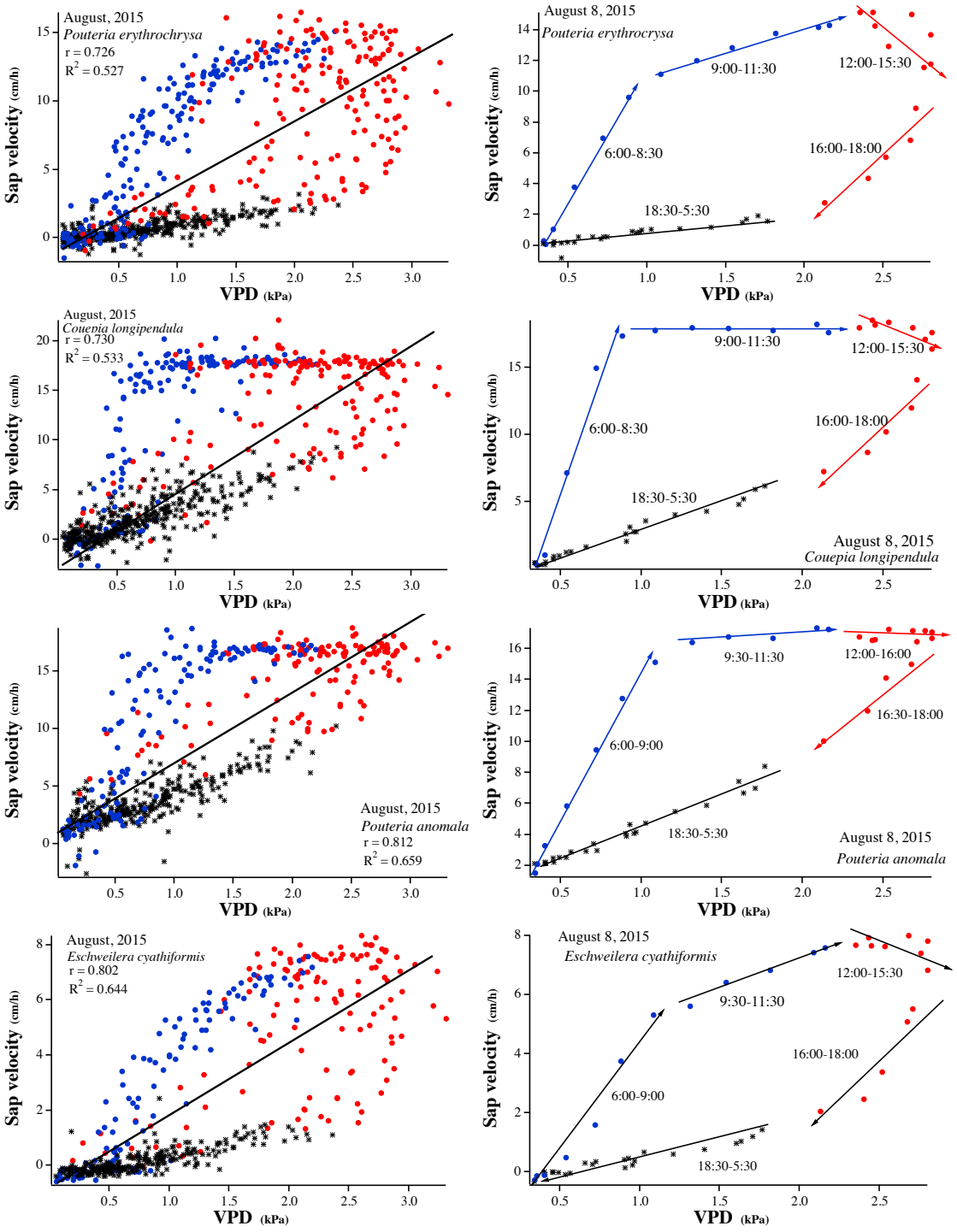

Figure 3. Relationship between sap velocity and vapor pressure deficit (VPD) for the species *Eschweilera cyathiformis*, *Pouteria anomala*, *Couepia longipendula* and *Pouteria erythrochrysa,* during the month of August, 2015 (left side) and during a daily cycle measured on August 8 of 2015 (right side, same day and time leaf water potential measurements were carried out). Day measurements (6:00-18:00) are represented by

circles and are divided into pre-noon (blue circles, 6:00-11:30) and post-noon (red circles, 12:00-18:00). Measurements made at night (18:30 – 5:30) are represented by black asterisks.

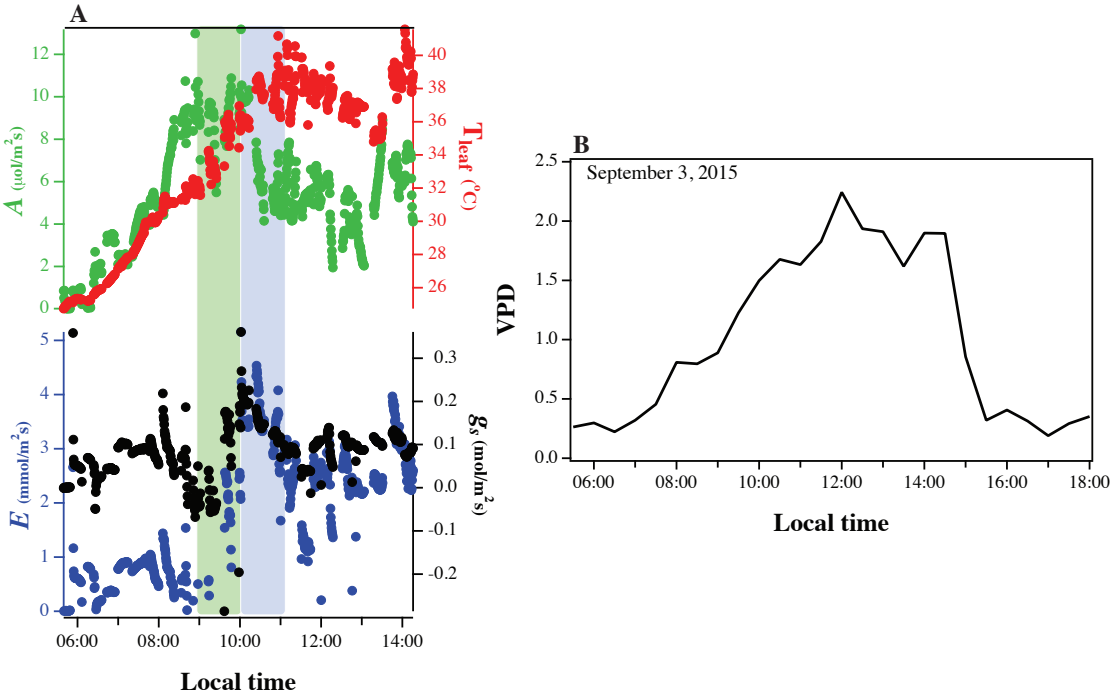

Figure 4. **(a)** - *In-situ* diurnal observations of leaf temperature T_{leaf}, net photosynthesis (A), transpiration (E), and stomatal conductance (g_s) from leaves of a *Pouteria anomala* branch in the upper canopy (25 m height) in the Central Amazon during September of 2015. Green box represents the peak of photosynthesis, and the blue is the peak of transpiration **(b)** – Diurnal vapor pressure deficit (VPD) measured at 35 m height during September 3 of 2015.